
MODIFIER ADAPTATION MEETS BAYESIAN OPTIMIZATION AND DERIVATIVE-FREE OPTIMIZATION

A PREPRINT

E. A. del Rio Chanona*

Department of Computer Science
Centre for Process Systems Engineering
Department of Chemical Engineering
Imperial College London, UK

P. Petsagkourakis*

Centre for Process Systems Engineering
Department of Chemical Engineering
University College London, UK

E. Bradford

Department of Engineering Cybernetics
Norwegian University of Science and Technology
Trondheim, Norway

J. E. Alves Graciano[†]

Universidade de São Paulo
Escola Politecnica
Departamento de Engenharia Química
São Paulo, Brazil

B. Chachuat[‡]

Department of Computer Science
Centre for Process Systems Engineering
Department of Chemical Engineering
Imperial College London, UK

ABSTRACT

This paper investigates a new class of modifier-adaptation schemes to overcome plant-model mismatch in real-time optimization of uncertain processes. The main contribution lies in the integration of concepts from the areas of Bayesian optimization and derivative-free optimization. The proposed schemes embed a physical model and rely on trust-region ideas to minimize risk during the exploration, while employing Gaussian process regression to capture the plant-model mismatch in a non-parametric way and drive the exploration by means of acquisition functions. The benefits of using an acquisition function, knowing the process noise level, or specifying a nominal process model are illustrated on numerical case studies, including a semi-batch photobioreactor optimization problem.

Keywords real-time optimization · modifier adaptation · trust region · Gaussian process regression · Bayesian optimization · model-free RTO

1 Introduction

The business benefits of real-time optimization (RTO) in the oil-and-gas and chemical sectors are not disputed (Darby et al., 2011; Câmara et al., 2016). Despite this, the deployment and penetration of this technology have remained relatively low. The causes for this are many, but in particular, companies invariably need to employ highly-qualified process control engineers to design, install and continually maintain RTO systems to preserve benefits. These systems rely on knowledge-driven (mechanistic) models, and in those processes where the optimization execution period is

*Equal contributors.

[†]Present address: Radix Engenharia e Software, Rio de Janeiro, Brazil

[‡]Corresponding author, b.chachuat@imperial.ac.uk

much longer than the closed-loop process dynamics, steady-state models are commonly employed to conduct the optimization (Marlin and Hrymak, 1997). Traditionally, the model is updated in real-time using process measurements, before repeating the optimization on a time-scale of hours to days. This two-step RTO scheme, often referred to as model-adaptation strategy, is both intuitive and popular but it can hinder convergence to a plant’s optimal operating point due to lack of integration between the model-update and optimization steps, especially in the presence of plant-model mismatch (Tatjewski, 2002; Gao and Engell, 2005; Tejada-Iglesias et al., 2019). This has fueled the development of alternative adaptation paradigms in RTO (Engell, 2007; Chachuat et al., 2009), such as modifier adaptation (Marchetti et al., 2009).

Similar to the two-step RTO scheme, modifier adaptation embeds the available process model into a nonlinear optimization problem that is solved on every RTO execution. The key difference is that the process measurements are now used to update the so-called modifiers that are added to the cost and constraint functions in the optimization model, while keeping a nominal process model. This methodology greatly alleviates the problem of offset from the actual plant optimum, by ensuring that the KKT conditions determined by the model match those of the plant upon convergence (Marchetti et al., 2009). However, this desideratum comes at the cost of having to estimate the cost and constraint gradients from process measurements.

Inferring gradient information from noisy process measurements is challenging, but nonetheless key to the effectiveness and reliability of modifier adaptation (Bunin et al., 2013; Jeong et al., 2018). Variants of the modifier-adaptation principle in order to mitigate this burden are surveyed by Marchetti et al. (2016). They include recursive update schemes that exploit past steady-state operating points (Gao and Engell, 2005; Marchetti et al., 2010; Rodger and Chachuat, 2011), selective adaptation schemes that rely on directional derivatives (Costello et al., 2016), as well as schemes that take advantage of transient process measurements (François and Bonvin, 2014; Krishnamoorthy et al., 2018; Speakman and François, 2020). Other variants do not require estimating plant gradients explicitly. The nested modifier-adaptation scheme by Navia et al. (2015) embeds the modified optimization model into an outer problem that optimizes over the gradient modifiers using a derivative-free algorithm. Gao et al. (2016) proposed to combine quadratic surrogates trained on available plant data with a nominal mechanistic model in order to account for curvature information and filter out the process noise. Likewise, Singhal et al. (2016) investigated data-driven approaches based on quadratic surrogates as modifiers for the predicted cost and constraint functions and devised an online adaptation strategy for the surrogates inspired by trust-region ideas. More recently, Ferreira et al. (2018) were the first to consider Gaussian processes (GP), trained from past measurement information, as the cost and constraint modifiers. Then del Rio-Chanona et al. (2019) developed this strategy further by introducing modifier-adaptation schemes that rely on trust regions to capture the GPs’ ability to capture the cost and constraint mismatch. But the theoretical properties and practical performance of these schemes are yet to be analyzed in greater depth.

The idea of correcting the mismatch of a knowledge-driven model with a data-driven model is akin to hybrid semi-parametric modeling (Thompson and Kramer, 1994; von Stosch et al., 2014), specifically a parallel hybrid model structure. The consideration of non-parametric models, whereby the nature and number of parameters is not determined by a priori knowledge but tailored to the data at hand, makes perfect sense to capture the structural plant-model mismatch in RTO applications. In principle, this approach is even amenable to a completely model-free RTO scheme by simply discarding the mechanistic model component. But the effect of removing this mechanistic knowledge in a practical RTO setup has seldom been investigated to date.

Model predictive control (MPC) is closely related to RTO in that these two technologies entail the repeated solution of a model-based optimization problem at their core (Rawlings et al., 2017). Similar to RTO, a majority of successful MPC implementations have so far relied on mechanistic models. But there has been a renewal of interest in data-driven approaches, which use surrogate models trained on historical data or mechanistic model simulations to drive the optimization. The type of surrogate models used in MPC include artificial neural networks (Piche et al., 2000; Wu et al., 2019) and GPs (Kocijan et al., 2004). However, comparatively little work has been published on embedding hybrid models into MPC in order to reduce the dependency on data and infuse physical knowledge for better extrapolation capability (Klimasauskas, 1998; Zhang et al., 2019).

A recent trend in MPC has been to include learning or self-reflective objectives alongside control performance objectives (Hewing et al., 2020). Self-reflective MPC seeks to minimize the controller’s own performance loss in the presence of uncertainty (Feng and Houska, 2018). Instead, learning objectives aim to promote accurate future state and parameter estimates, inspired by optimal experiment design or persistent excitation ideas (Larsson et al., 2013; Heirung et al., 2015; Marafioti et al., 2014). In data-driven MPC for instance, recent research has investigated on-line learning of the surrogates to improve performance and reliability, with a particular interest in GPs (Maiworm et al., 2018; Bradford et al., 2019, 2020). In essence, MPC with learning seeks to strike a balance between exploitation against exploration, which is akin to the dual control problem (Wittenmark, 1995) and is also the central paradigm in the fast-developing field of reinforcement learning (Spielberg et al., 2019; Kim et al., 2020; Petsagkourakis et al.,

2020b,a,c). Likewise, several modifier-adaptation schemes have incorporated excitation terms in the constraints of the RTO model in order to enable more accurate gradient estimates from noisy measurements (Marchetti et al., 2010; Rodger and Chachuat, 2011). But the vast potential of machine learning and reinforcement learning has remained largely untapped in the RTO context (Powell et al., 2020).

Other areas closely related to real-time optimization comprise black-box optimization and surrogate-based optimization, which find many applications in process flowsheeting, computational fluid dynamics, or molecular dynamics (Biegler et al., 2014). They can be broadly classified into local and global approaches. Global approaches proceed by constructing a surrogate model based on an ensemble of simulations before optimizing it, often within an iteration where the surrogate is progressively refined. A number of practical implementations rely on neural networks (Henao and Maravelias, 2011), GPs (Caballero and Grossmann, 2008; Quirante et al., 2015; Keßler et al., 2019), or a combination of various basis functions (Wilson and Sahinidis, 2017; Boukouvala and Floudas, 2017) for the surrogate modeling. Bayesian optimization has gained significant popularity for tackling problems with expensive function evaluations, with prominent algorithms such as efficient global optimization (Jones et al., 1998) and sequential kriging optimization (Huang et al., 2006) that leverage GP surrogates and so-called acquisition functions to strike a balance between exploitation and exploration. Radial basis function (RBF) surrogates have also proven effective to optimize expensive black-box function (Gutmann, 2001; Costa and Nannicini, 2018). Handling constrained problems with this class of methods constitutes an active field of research nonetheless (Audet et al., 2018; Cartis et al., 2018).

By contrast, local approaches maintain an accurate approximation of the original optimization problem within a trust region, whose position and size are adapted iteratively. This procedure entails updating or reconstructing the surrogate model as the trust region moves around, but it benefits from a well-developed convergence theory providing sufficient conditions for local optimality in unconstrained and bound-constrained problems (Conn et al., 2000, 2009b; March and Willcox, 2012b; Cartis et al., 2019). Extensions of these approaches to constrained flowsheet optimization include the work by Eason and Biegler (2016, 2018) and Bajaj et al. (2018), while constrained multi-fidelity optimization was considered by March and Willcox (2012a). In particular, the latter uses GP surrogates as low-fidelity models and their adaptation is akin to modifier adaptation with GP surrogates as developed by Ferreira et al. (2018) and del Rio-Chanona et al. (2019). These connections between the modifier-adaptation and trust-region frameworks were also delineated in a short note by Bunin (2014). But while integrating local and global concepts from surrogate-based optimization methods within modifier adaptation is indeed appealing, this integration should account for the added complexity posed by noisy process data or changing optima over time in RTO.

Considering all this, the main focus of this paper is on improving modifier-adaptation schemes in terms of speed and reliability by integrating concepts and ideas from the areas of Bayesian optimization and derivative-free optimization. Specifically, the proposed modifier-adaptation schemes embed a physical model and trust-region concepts to minimize risk during the exploration, while relying on GPs to capture the plant-model mismatch in a non-parametric way and drive the exploration by means of acquisition functions. Key elements of novelty include the adaptation of the trust region based on the GPs' mean predictor ability to capture the plant-model mismatch in the cost and constraints and the exploitation of the GPs' variance estimators to maintain sufficient excitation during the search. We furthermore investigate the effect of removing the prior, knowledge-based model component and the effect of process noise by means of numerical examples. The rest of the paper provides background on MA and GP in Sec. 2, then presents and analyses the new modifier-adaptation algorithm in Section 3. This algorithm is illustrated with a simple quadratic optimization problem throughout Section 3 and with practical case studies in Section 4, before drawing final remarks in Section 5.

2 Preliminaries

2.1 Modifier Adaptation

The problem of optimizing the steady-state performance of a given plant subject to operational or safety constraints can be formulated as:

$$\begin{aligned} \min_{\mathbf{u} \in \mathcal{U}} G_0^{\text{P}}(\mathbf{u}) &:= g_0(\mathbf{u}, \mathbf{y}^{\text{P}}(\mathbf{u})) \\ \text{s.t. } G_i^{\text{P}}(\mathbf{u}) &:= g_i(\mathbf{u}, \mathbf{y}^{\text{P}}(\mathbf{u})) \leq 0, \quad i = 1 \dots n_g \end{aligned} \quad (1)$$

where $\mathbf{u} \in \mathbb{R}^{n_u}$ and $\mathbf{y}^{\text{P}} \in \mathbb{R}^{n_y}$ are vectors of the plant input and output variables, respectively; $g_i : \mathbb{R}^{n_u} \times \mathbb{R}^{n_y} \rightarrow \mathbb{R}$, $i = 0, \dots, n_g$, denote the cost and inequality constraint functions; and $\mathcal{U} \subseteq \mathbb{R}^{n_u}$ is the control domain, e.g. lower and upper bounds on the input variables, $\mathbf{u}^{\text{L}} \leq \mathbf{u} \leq \mathbf{u}^{\text{U}}$. Notice the superscript $(\cdot)^{\text{P}}$ used to indicate plant-related quantities.

The RTO challenge is of course that an exact mapping $\mathbf{y}^p(\cdot)$ is unknown in practice, and the output $\mathbf{y}^p(\mathbf{u})$ can only be measured for a particular input value \mathbf{u} , in the manner of a noisy oracle. However, provided that a non-ideal (approximate) model of the plant's input-output behavior is available, represented by the parametric function $\mathbf{y}(\mathbf{u}, \cdot)$, one may solve the following model-based optimization problem instead:

$$\begin{aligned} \min_{\mathbf{u} \in \mathcal{U}} G_0(\mathbf{u}) &:= g_0(\mathbf{u}, \mathbf{y}(\mathbf{u}, \boldsymbol{\theta})) \\ \text{s.t. } G_i(\mathbf{u}) &:= g_i(\mathbf{u}, \mathbf{y}(\mathbf{u}, \boldsymbol{\theta})) \leq 0, \quad i = 1 \dots n_g \end{aligned} \quad (2)$$

where $\boldsymbol{\theta} \in \mathbb{R}^{n_\theta}$ is a vector of adjustable model parameters.

In the presence of plant-model mismatch and process disturbances, the optimal solution value of Problem (2) could be significantly different from that of Problem (1). For this reason, a traditional two-step RTO scheme would try to reduce the plant-model mismatch by adjusting (a subset of) the model parameters with new plant measurements collected at each iteration. However, the convergence of such a scheme to a plant optimum is dependent upon a model adequacy condition (Forbes et al., 1994), whereby the model and plant optima match for at least one set of parameter values.

By contrast, the measurements in a modifier-adaptation scheme are used to correct the cost and constraint function values at a given iterate \mathbf{u}^k , in order to determine the next input or set-point values \mathbf{u}^{k+1} (Marchetti et al., 2009):

$$\begin{aligned} \mathbf{u}^{k+1} \in \arg \min_{\mathbf{u} \in \mathcal{U}} G_0(\mathbf{u}) + (\boldsymbol{\lambda}_{G_0}^k)^\top \mathbf{u} \\ \text{s.t. } G_i(\mathbf{u}) + \varepsilon_{G_i}^k + (\boldsymbol{\lambda}_{G_i}^k)^\top [\mathbf{u} - \mathbf{u}^k] \leq 0, \quad i = 1 \dots n_g \end{aligned} \quad (3)$$

where $\varepsilon_{G_i}^k \in \mathbb{R}$ are zeroth-order modifiers for the constraints, and $\boldsymbol{\lambda}_{G_i}^k \in \mathbb{R}^{n_u}$ are first-order modifiers for the cost and constraints. The use of modifiers is appealing in that a KKT point \mathbf{u}^∞ for the corrected model-based problem (3) is also a KKT point for the original problem (1), provided that the modifiers satisfy (Marchetti et al., 2009):

$$\begin{aligned} \varepsilon_{G_i}^k &= G_i^p(\mathbf{u}^\infty) - G_i(\mathbf{u}^\infty), \quad i = 1 \dots n_g \\ \boldsymbol{\lambda}_{G_i}^k &= \nabla G_i^p(\mathbf{u}^\infty) - \nabla G_i(\mathbf{u}^\infty), \quad i = 0 \dots n_g \end{aligned}$$

A simple update rule for the modifiers that fulfills the foregoing conditions upon convergence is:

$$\begin{aligned} \varepsilon_{G_i}^{k+1} &= (1 - \eta)\varepsilon_{G_i}^k + \eta [G_i^p(\mathbf{u}^k) - G_i(\mathbf{u}^k)] \\ \boldsymbol{\lambda}_{G_i}^{k+1} &= (1 - \eta)\boldsymbol{\lambda}_{G_i}^k + \eta [\nabla G_i^p(\mathbf{u}^k) - \nabla G_i(\mathbf{u}^k)] \end{aligned} \quad (4)$$

where the tuning parameters $\eta \in (0, 1]$ may be reduced to help stabilize the iterations. Apart from choosing a suitable η , the biggest burden with this approach is estimating the gradients $\nabla G_i^p(\mathbf{u}^k)$ of the cost and constraint functions at each RTO iteration. A range of methods were reviewed in the paper's introduction to assist with this estimation.

2.2 Gaussian Processes and Acquisition Functions

GP regression is a method of interpolation developed by Krige (1951) and popularized by the machine learning community (Rasmussen and Williams, 2016). It aims to describe an unknown function $f : \mathbb{R}^{n_u} \rightarrow \mathbb{R}$ using noisy observations, $y = f(\mathbf{u}) + \nu$, where $\nu \sim \mathcal{N}(0, \sigma_\nu^2)$ is Gaussian distributed measurement noise with zero mean and (possibly unknown) variance σ_ν^2 . GPs themselves consider a distribution over functions and may be regarded as a generalization of multivariate Gaussian distributions:

$$f(\cdot) \sim \mathcal{GP}(m(\cdot), k(\cdot, \cdot))$$

where the mean function $m(\cdot)$ can be interpreted as the deterministic part of the function; and the covariance function $k(\cdot, \cdot)$ accounts for correlations between the function values at different points.

One popular choice for the covariance function is the squared-exponential (SE) kernel (Rasmussen and Williams, 2016):

$$k(\mathbf{u}, \mathbf{u}') := \sigma_n^2 \exp\left(-\frac{1}{2}(\mathbf{u} - \mathbf{u}')^\top \boldsymbol{\Lambda}(\mathbf{u} - \mathbf{u}')\right)$$

where σ_n^2 is the covariance magnitude; and $\boldsymbol{\Lambda} := \text{diag}(\lambda_1 \dots \lambda_{n_u})$ is a scaling matrix. Underlying this kernel choice is the assumption that the inferred function f is both smooth and stationary. But other kernels could of course be selected, such as the Matérn class of covariance functions (Rasmussen and Williams, 2016). We furthermore choose a constant mean function:

$$m(\mathbf{u}) := c$$

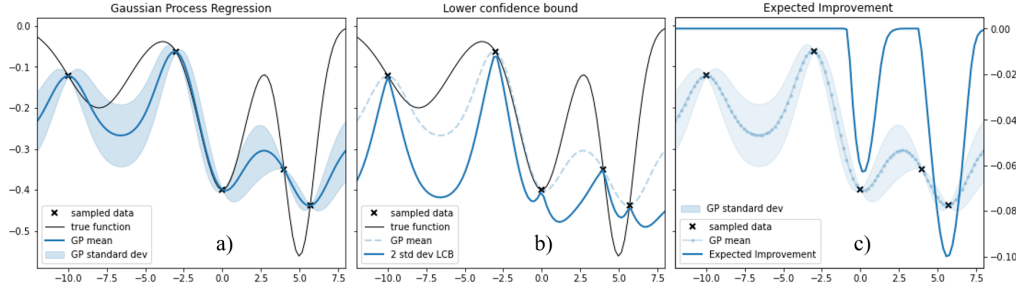


Figure 1: (a) Illustration of the posterior mean and variance functions in the Gaussian process regression of a sampled function (Equation 5). (b) Corresponding lower confidence bound (LCB) acquisition function (Equation 6). (c) Corresponding expected improvement (EI) acquisition function (Equation 7).

where c is the scalar offset. This choice is motivated by the fact that since GPs are used to describe the plant-model mismatch in modifier adaptation, it is safe for their predictions to tend to a constant offset when extrapolating away from the measurement points.

Maximum likelihood estimation is commonly applied to infer a GP’s hyperparameters $\Psi := [c \ \sigma_n \ \sigma_\nu \ \lambda_1 \ \dots \ \lambda_{n_u}]^\top$, where σ_ν may be excluded in case the measurement noise variance is known. Consider N (noisy) function observations, denoted by $\mathbf{y} := [y_1 \ \dots \ y_N]^\top \in \mathbb{R}^N$, with corresponding inputs gathered in the matrix $\mathbf{U} := [\mathbf{u}_1 \ \dots \ \mathbf{u}_N] \in \mathbb{R}^{n_u \times N}$. The log-likelihood of the observed data, ignoring constant terms, is given by:

$$\mathcal{L}(\Psi) := -\frac{1}{2} \ln(|\mathbf{K}(\mathbf{U})|) - \frac{1}{2} (\mathbf{y} - \mathbf{1}c)^\top \mathbf{K}(\mathbf{U})^{-1} (\mathbf{y} - \mathbf{1}c)$$

with $K_{ij}(\mathbf{U}) := k(\mathbf{u}_i, \mathbf{u}_j) + \sigma_\nu^2 \delta_{ij}$ for all $(i, j) \in \{1 \dots N\}^2$; and Kronecker’s delta function δ_{ij} .

The predicted distribution of $f(\mathbf{u})$ at an arbitrary input point \mathbf{u} , given the input-output data (\mathbf{U}, \mathbf{y}) and the maximum-likelihood estimates of Ψ , follows a Gaussian distribution:

$$f(\mathbf{u}) \mid \mathbf{U}, \mathbf{y} \sim \mathcal{N}(\mu_f(\mathbf{u}), \sigma_f^2(\mathbf{u})) \quad (5)$$

where the posterior mean function μ_f and the posterior variance function σ_f^2 are computed as:

$$\begin{aligned} \mu_f(\mathbf{u}) &:= \mathbf{r}(\mathbf{u}, \mathbf{U}) \mathbf{K}(\mathbf{U})^{-1} \mathbf{y} + c \\ \sigma_f^2(\mathbf{u}) &:= \sigma_n^2 - \mathbf{r}(\mathbf{u}, \mathbf{U}) \mathbf{K}(\mathbf{U})^{-1} \mathbf{r}(\mathbf{u}, \mathbf{U})^\top \end{aligned}$$

with $\mathbf{r}(\mathbf{u}, \mathbf{U}) := [k(\mathbf{u}, \mathbf{u}_1) \ \dots \ k(\mathbf{u}, \mathbf{u}_N)]$.

In practice, the mean μ_f corresponds to the GP’s prediction at \mathbf{u} , while the variance σ_f^2 provides a measure of the uncertainty associated to this prediction (Figure 1a). Both functions are exploited in so-called acquisition functions, which constitute the workhorse of Bayesian estimation in balancing exploration versus exploitation (Shahriari et al., 2016). Two popular acquisition functions are reviewed next, namely *lower confidence bound* (LCB) and *expected improvement* (EI). These will be considered later as objective functions in the optimization subproblems of the modifier-adaptation algorithm. Alternative acquisition functions include *probability of improvement* (Kushner, 1964), *knowledge gradient* (Frazier et al., 2009), and *entropy search* (Hennig and Schuler, 2012) to name but a few.

Lower Confidence Bound With the notation introduced previously (Equation 5), this acquisition function is given by (Figure 1b):

$$\mathcal{A}_{\text{LCB}}[\mu_f, \sigma_f](\mathbf{u}) := \mu_f(\mathbf{u}) - \beta \sigma_f(\mathbf{u}) \quad (6)$$

where β may be interpreted as an exploration weight. Notice the negative sign of the exploration term in Equation (6), which is consistent with the formulation of the RTO Problem (1) as a minimization. The LCB function is based on the principle of optimism in the face of uncertainty, with a view to minimizing regret. Its early use can be traced back to the work by Lai and Robbins (1985) on rule allocations, and later by Agrawal (1995) in the context of reinforcement learning.

Expected Improvement This acquisition function is expressed as (Figure 1c):

$$\mathcal{A}_{\text{EI}}[\mu_f, \sigma_f, f_L](\mathbf{u}) := -[f_L - \mu_f(\mathbf{u})] \Phi\left(\frac{f_L - \mu_f(\mathbf{u})}{\sigma_f(\mathbf{u})}\right) - \sigma_f(\mathbf{u}) \phi\left(\frac{f_L - \mu_f(\mathbf{u})}{\sigma_f(\mathbf{u})}\right) \quad (7)$$

where $\phi(\cdot)$ and $\Phi(\cdot)$ are the standard normal probability density and cumulative distribution functions, respectively; and $f_L := \min(y_1, \dots, y_N)$ is the best observed value, possibly replaced with the lowest mean value, $\min(\mu_f(\mathbf{u}_1), \dots, \mu_f(\mathbf{u}_N))$, in case the observations carry significant noise. This expression corresponds to $\mathbb{E}[\max(f_L - \mu_f(\cdot), 0)]$, where the improvement function $\max(f_L - \mu_f(\cdot), 0)$ is only positive at points where the predicted mean value is lower than f_L . The negative signs are introduced so that \mathcal{A}_{EI} can be used as objective function in a minimization problem, rather than maximized. Its introduction is credited to Moćkus (1975) and it was later popularized via the efficient global optimization (EGO) algorithm by Jones et al. (1998).

Both the LCB and EI acquisition functions seek to balance exploration and exploitation in order to reduce the overall number of observations. Computational benchmarks tend to favor EI over LCB though, since the latter may lead to excessive exploration (Snoek et al., 2012; Shahriari et al., 2016). Nevertheless, there are theoretically motivated guidelines for tuning the weight β to achieve optimal regret (Srinivas et al., 2010), and thereby boost the performance of USB. Both functions furthermore come with caveats in practice, as LCB typically comprises a larger number of local optima, whereas EI can present large flat areas. These characteristics call for randomized search or complete search approaches in applications (see, e.g. Törn and Žilinskas, 1989; Schweidtmann et al., 2020).

3 Methodology

3.1 Modifier-Adaptation Algorithm Statement

The use of GPs to describe the plant-model mismatch in an RTO problem was first proposed by Ferreira et al. (2018). The main idea was for these GP modifiers to correct the cost and each constraint separately:

$$G_i^p - G_i \sim \mathcal{GP}(\mu_{\delta G_i}, \sigma_{\delta G_i}^2), \quad i = 0 \dots n_g$$

The following modified optimization problem was then solved in an RTO iteration:

$$\begin{aligned} \mathbf{u}^{k+1} \in \arg \min_{\mathbf{u} \in \mathcal{U}} [G_0 + \mu_{\delta G_0}^k](\mathbf{u}) \\ \text{s.t. } [G_i + \mu_{\delta G_i}^k](\mathbf{u}) \leq 0, \quad i = 1 \dots n_g \end{aligned} \quad (8)$$

where $\mu_{\delta G_i}^k$ denotes the mean of the GP trained with the input-output data set $(\mathbf{U}^k, \delta \mathbf{G}_i^k)$; and $\delta \mathbf{G}_i^k$ comprises measurements of the mismatch $\delta G_i(\cdot) := G_i^p(\cdot) - G_i(\cdot)$ for inputs in the matrix \mathbf{U}^k . This idea of constructing GP surrogates for the cost and constraint black-box functions is also shared by various derivative-free algorithms (March and Willcox, 2012a; Picheny et al., 2016).

Herein, we revisit this idea by introducing trust-region concepts from the fields of derivative-free and surrogate-based optimization together with acquisition functions from Bayesian optimization. The modified optimization problem that is solved at each RTO iteration becomes:

$$\begin{aligned} \mathbf{d}^{k+1} \in \arg \min_{\mathbf{d}} \mathcal{A}[G_0 + \mu_{\delta G_0}^k, \sigma_{\delta G_0}^k, \cdot](\mathbf{u}^k + \mathbf{d}) \\ \text{s.t. } [G_i + \mu_{\delta G_i}^k](\mathbf{u}^k + \mathbf{d}) \leq 0, \quad i = 1 \dots n_g \\ \|\mathbf{d}\| \leq \Delta^k, \quad \mathbf{u}^k + \mathbf{d} \in \mathcal{U} \end{aligned} \quad (9)$$

where $\Delta^k \geq 0$ is the trust-region radius for the predicted step $\mathbf{d}^{k+1} \in \mathbb{R}^{n_u}$; and \mathcal{A} is an acquisition function for the cost predictor $G_0 + \mu_{\delta G_0}^k$ and the associated error estimate $\sigma_{\delta G_0}^k$, which may be either the LCB or EI function (cf. Section 2.2) or the cost predictor itself if exploration is not considered.

Solving Problem (9) is akin to conducting a constrained Bayesian optimization within a trust-region. The various steps used to adapt this trust region and handle the constraints are summarized in Algorithm 1 and commented below.

Initialization A set of GPs are trained on cost and constraint mismatch data in the initial step. There is considerable freedom regarding the choice of this initial training set $(\mathbf{U}^0, \delta \mathbf{G}_i^0)$, $i = 0 \dots n_g$ as well as the initial trust-region center \mathbf{u}^0 and radius Δ^0 . One approach entails defining the initial trust region first, then selecting an initial sample set within this trust region in a second step. Such an initial trust region may leverage process knowledge and physical insight in practice. Identifying a feasible starting point for (a subset of) the process constraints could also be via the solution of an auxiliary feasibility problem prior to running Algorithm 1 (Bajaj et al., 2018). Sample points may then be generated within this trust region by imposing finite perturbations along each input direction or using quasi-random sampling, ideally so that the GP surrogates can be certified to be fully linear—further discussions of the full linearity property

Algorithm 1 Modifier adaptation with Gaussian process, trust region and acquisition function

Input: initial data sets $(\mathbf{U}^0, \delta \mathbf{G}_i^0)$, $i = 0 \dots n_g$; trained GP modifiers $\mu_{\delta G_i}^0$, $i = 0 \dots n_g$ and $\sigma_{\delta G_0}^0$; initial operating point $\mathbf{u}^0 \in \mathcal{U}$; initial and maximal trust-region radii $0 < \Delta^0 < \Delta_{\max}$; trust-region parameters $0 < \eta_1 < \eta_2 < 1$, $0 < \gamma_{\text{red}} < 1 < \gamma_{\text{inc}}$, and $\mu > 0$; subset of unrelaxable constraints $\mathcal{UC} \subseteq \{1 \dots n_g\}$

Repeat: for $k = 0, 1, \dots$

1. Check criticality
If $\Delta^k > \mu \|\nabla_{\text{red}}[G_0 + \mu_{\delta G_0}^k](\mathbf{u}^k)\|$: $\Delta^k \leftarrow \gamma_{\text{red}} \Delta^k$
2. Solve modified optimization problem (Equation 9) $\triangleright \mathbf{d}^{k+1}$
3. Get process cost and constraint measurements $\triangleright G_i^p(\mathbf{u}^k + \mathbf{d}^{k+1}), i = 0 \dots n_g$
4. Check infeasibility
If Problem (9) is infeasible or $G_i^p(\mathbf{u}^k + \mathbf{d}^{k+1}) > 0$ for any $i \in \mathcal{UC}$:
 $\Delta^{k+1} \leftarrow [\gamma_{\text{red}}, 1] \Delta^k$, $\mathbf{u}^{k+1} \leftarrow \mathbf{u}^k$ (reject), and goto Step 7
5. Compute merit function (Equation 10) $\triangleright \rho^{k+1}$
6. Update trust region
If $\rho^{k+1} > \eta_2 \wedge \|\mathbf{d}^{k+1}\| = \Delta^k$: $\Delta^{k+1} \leftarrow \gamma_{\text{inc}} \Delta^k$, $\mathbf{u}^{k+1} \leftarrow \mathbf{u}^k + \mathbf{d}^{k+1}$ (accept)
Else If $\rho^{k+1} < \eta_1$: $\Delta^{k+1} \leftarrow \gamma_{\text{red}} \Delta^k$, $\mathbf{u}^{k+1} \leftarrow \mathbf{u}^k$ (reject)
Else: $\Delta^{k+1} \leftarrow \Delta^k$, $\mathbf{u}^{k+1} \leftarrow \mathbf{u}^k + \mathbf{d}^{k+1}$ (accept)
7. Update data sets $\triangleright (\mathbf{U}^{k+1}, \delta \mathbf{G}_i^{k+1}), i = 0 \dots n_g$
8. Update GP modifiers $\triangleright \mu_{\delta G_i}^{k+1}, i = 0 \dots n_g; \sigma_{\delta G_0}^{k+1}$

are deferred to the convergence subsection below. When a process data set $(\mathbf{U}^0, \delta \mathbf{G}_i^0)$, $i = 0 \dots n_g$ is preexisting, such as historical data, another approach involves constructing a maximal trust region that lies within a confidence percentile of the cost and constraint GP predictors $(\mu_{\delta G_i}^0, \sigma_{\delta G_i}^0)$ trained on this data set. Although such maximization problems are generally hard to solve because of their nonconvexity, good feasible solutions may nevertheless be obtained for practical purposes with any local solver and a multistart heuristic or using any global solver as feasibility pump (Schweidtmann et al., 2020).

The issue of scaling is closely related to that of trust-region and GP initialization. In practice, one can exploit the input domain \mathcal{U} to scale the input variable to within $[0, 1]$. The benefits of operating within a scaled input domain, both in terms of trust-region adaptation and GP training, are clear. A maximal trust-region radius may also be defined more conveniently in a scaled input domain, e.g. $\Delta_{\max} = 0.7$. Note that there is furthermore considerable flexibility in the choice of the trust region parameters $\eta_1, \eta_2, \gamma_{\text{red}}$ and γ_{inc} . A common setting in trust-region methods, which is also the setting used for the numerical case studies below, is $\eta_1 = 0.2, \eta_2 = 0.8, \gamma_{\text{red}} = 0.8$ and $\gamma_{\text{inc}} = 1.2$. By contrast, the criticality parameter μ is problem dependent and may be set to an arbitrary large value if shrinking of the trust region upon convergence to a stationary point is not desirable.

Adaptation Mechanisms The trust region serves the dual purpose of restricting the step size to the neighborhood where the cost and constraint surrogates are deemed to be predictive, while also defining the neighborhood in which the points are sampled for the construction of these surrogates. The trust region update corresponds to Steps 1, 4 and 6 of Algorithm 1. The latter comprises the classical update rules in trust-region algorithms (Conn et al., 2009b), which is based on the ratio of actual cost reduction to predicted cost reduction:

$$\rho^{k+1} := \frac{G_0^p(\mathbf{u}^k) - G_0^p(\mathbf{u}^k + \mathbf{d}^{k+1})}{[G_0 + \mu_{\delta G_0}^k](\mathbf{u}^k) - [G_0 + \mu_{\delta G_0}^k](\mathbf{u}^k + \mathbf{d}^{k+1})} \quad (10)$$

The trust-region radius Δ^{k+1} is reduced whenever the accuracy ratio ρ^{k+1} is too low. Conversely, Δ^{k+1} is increased if the optimization model (9) takes a full step and the modified cost is deemed a good enough prediction of the plant cost variation around this point. Otherwise, the trust-region radius stays unchanged. As for the operating point update, the full step \mathbf{d}^{k+1} is accepted when the accuracy ratio ρ^{k+1} is large enough. Otherwise, the operating point remains unchanged, which would entail a back-tracking in a practical RTO setup.

Before applying these updates, Step 4 asserts the feasibility of the modified optimization model (9) and of the plant constraints. Any infeasibility triggers a rejection of the step \mathbf{d}^{k+1} and a possible reduction of the trust-region radius,

again resulting in backtracking to point \mathbf{u}^k in a practical RTO setup. Note that such a strategy also requires that the initial point \mathbf{u}^0 should satisfy all the plant constraints. Backtracking is equivalent to the extreme-barrier approach in the trust-region literature (Audet and Dennis, 2006; Conn et al., 2009b; Larson et al., 2019), which assigns an infinite cost to points that violate any constraint. It is also customary in this literature to distinguish between relaxable and unrelaxable constraints, where only the former may be violated along the search path. Various approaches to handling relaxable constraints within trust-region algorithms have been developed in recent years, including progressive-barrier, augmented-Lagrangian and filter methods (see, e.g. Picheny et al., 2016; Larson et al., 2019). Integrating these techniques within a modifier-adaptation scheme is promising, but falls beyond the scope of the present paper. Instead, we shall only apply backtracking to the unrelaxable constraints subsequently (subset \mathcal{UC}), while bypassing this check for the relaxable inequality or equality constraints.

The criticality test in Step 1 is inspired by state-of-the-art trust-region algorithms in derivative-free optimization. The aim is to keep the radius of the trust region comparable to some measure of stationarity in order for the surrogate model to become more accurate as the iterates get closer to a stationary point. The update of the trust-region radius in Step 1 forces it to converge to zero, hence defining a natural stopping criterion for this class of methods (Conn et al., 2009b). In the presence of constraints, stationarity of the cost function may be substituted by Lagrangian stationarity or, alternatively, a reduced-gradient condition with:

$$\nabla_{\text{red}}[G_0 + \mu_{\delta G_0}^k](\mathbf{u}^k) := \nabla[G_0 + \mu_{\delta G_0}^k](\mathbf{u}^k) \mathbf{N}^k \quad (11)$$

where the columns of $\mathbf{N}^k \in \mathbb{R}^{n_u \times (n_u - n_{g,a})}$ form an orthogonal basis of the nullspace of the active constraint gradients at \mathbf{u}^k . However, it is better to treat this step as optional in a practical RTO setup, e.g. by allowing $\mu \rightarrow \infty$. This is because convergence of the trust-region radius to zero might hinder an RTO system’s capability to react to process disturbances in order to track a time-varying optimum.

Apart from updating the trust region, both the data sets and the GP modifiers are updated at Steps 7 and 8, irrespective of whether the step \mathbf{d}^{k+1} is accepted or not. The default strategy herein is to keep all of the past iterates and reconstruct the GPs by fitting all of their respective hyperparameters. In order to prevent overfitting and numerical difficulties in constructing the GPs, Ferreira et al. (2018) proposed to keep a limited number of historical records in the input-output data set. This subset could comprise the N most recent iterates or the N nearest-neighbors to the next operating point \mathbf{u}^{k+1} . The former is akin to a forgetting strategy that is suitable for the tracking of a changing optimum, while the latter might be more appropriate to precisely locate a steady optimum. Moreover, the current iterate \mathbf{u}^{k+1} need not be included in \mathbf{U}^{k+1} should it be within a given radius of an existing point in \mathbf{U}^k , or \mathbf{u}^{k+1} could be substituted for an existing nearby point in \mathbf{U}^{k+1} instead. The computational burden of reconstructing the GPs at each iteration could furthermore be eased upon updating the covariance matrix at certain iterations only (Rasmussen and Williams, 2016). Another key RTO design decisions is whether to identify the measurement noise variance σ_v^2 alongside the other GP hyperparameters (cf. Section 2.2), or to use an a priori noise variance provided by the sensor manufacturer or estimated from historical data. This discussion is deferred until the numerical analysis in Section 3.2.

Convergence and Performance Aspects The modifier-adaptation scheme in Algorithm 1 is inspired by the derivative-free trust-region method in Conn et al. (2009b, Algorithm 10.1). The benefit of this design is that Algorithm 1 is globally convergent to a first-order critical point for unconstrained problems, upon imposing additional conditions such as full linearity of the surrogates in each trust-region subproblem and in the absence of noise; this convergence analysis is reported in Appendix A for completeness. Derivative-free trust-region methods that are provably convergent for problems with black-box constraints have also been developed in recent years (Augustin and Marzouk, 2014; Echebest et al., 2017; Audet et al., 2018). These methods are based on full-linearity assumptions as well.

Derivative-free trust-region methods can be broadly classified into two categories, those which target good practical performance and those for which convergence is established (Conn et al., 2009b). The latter typically pay the price of practicality since ensuring full-linearity often requires taking extra sample points within the active trust region. This trade-off between convergence and performance is particularly relevant in the RTO context, whereby moving towards a process optimum sufficiently fast can be critical. With this in mind and the fact that the optimum can change due to process disturbances we do not enforce full linearity of the GP surrogates in Algorithm 1 and implement a simple backtracking strategy to handle constraint violation instead. Both the illustrative example in Section 3.2 and the numerical case study in Section 4 below confirm that Algorithm 1 can locate constrained process optima both efficiently and reliably, even in the presence of noise.

Without enforcing full linearity of the surrogates, however, a derivative-free trust-region algorithm may get trapped around a suboptimal point. We show with an illustrative example below (cf. Figures 2a & 2d) that Algorithm 1 may indeed fail to steer the iterates to a process optimum when the cost and constraints are simply corrected in the manner of Problem (8) in Step 2. A similar situation is known to occur in modifier-adaptation schemes that exploit past operating points in recursive gradient updates (Marchetti et al., 2010; Rodger and Chachuat, 2011), where the addition of extra

constraints in the RTO model to generate excitation can help mitigate the problem. Herein, we address this problem by leveraging ideas from Bayesian optimization for the first time. In particular, we use an acquisition function in order to promote exploration within the trust region (Problem 9). The acquisition functions of interest, lower confidence bound (LCB) and expected improvement (EI), were described in Section 2.2 and are assessed on an illustrative example in Section 3.2. Acquisition functions could also be considered for the constraints of the RTO model themselves, either to prevent constraint violation or to improve the accuracy of the constraint GP surrogates (Picheny et al., 2016; del Rio-Chanona et al., 2019), although this falls beyond the scope of the present paper.

Computational Aspects Traditional RTO systems often comprise complex numerical optimization subproblems as they rely on mechanistic models to drive the optimization. Correcting the cost and constraint functions with GP modifiers as in Problem (9) can introduce further nonlinearity and nonconvexity, thereby adding even more to this complexity. It is well known in particular that both the LCB and EI acquisition functions can exhibit a large number of local optima (cf. Figure 1). The application of global optimization methods is only computationally tractable for small-scale problems in practice (Schweidtmann et al., 2020). Instead, the numerical case studies throughout this paper are solved using a local solver in combination with a multistart heuristic. The corresponding python codes are made available in the Supporting Information for the sake of reproducibility.

In principle, one could also decide to construct the GP modifiers from scratch, that is, without correcting an a priori mechanistic model. The optimization subproblems in such a model-free RTO system could be solved to guaranteed global optimality more efficiently using state-of-the-art complete-search algorithms (Schweidtmann et al., 2020). But the lack of a mechanistic model embedded into the optimization problem might significantly slow down the progress of the iterates to a plant optimum or be detrimental to the reliability of the RTO system. This trade-off is analyzed in greater details in the following section and later illustrated on the case studies too.

3.2 Algorithm Performance and Analysis: Illustrative Example

We now analyze the performance of Algorithm 1 for various design choices by considering the following simple optimization problem:

$$\begin{aligned} \min_{\mathbf{u} \in [-2, 2]^2} \quad & y_1(\mathbf{u}) \\ \text{s.t.} \quad & y_2(\mathbf{u}) \leq 0 \\ & y_1(\mathbf{u}) := u_1^2 + u_2^2 + \theta_1 u_1 u_2 \\ & y_2(\mathbf{u}) := 1 - u_1 + u_2^2 + \theta_2 u_2 \end{aligned} \tag{12}$$

The (unknown) plant parameter values are taken as $\boldsymbol{\theta}^p = [1 \ 2]^\top$. The corresponding plant optimum (and the only KKT point here) is $\mathbf{u}^* \approx [0.368 \ -0.393]^\top$, where the inequality constraint is active and the optimal cost is $y_1^* \approx 0.145$. In order to conduct the RTO, we assume that both outputs y_1^p and y_2^p are measured and we add a Gaussian white noise of variance $\sigma_{y_1}^2 = \sigma_{y_2}^2 = 10^{-3}$ to the simulated values. Unless otherwise noted, we assume that the level of noise is not known a priori and therefore the variances $\sigma_{y_1}^2$ and $\sigma_{y_2}^2$ need to be estimated alongside the other GP hyperparameters (cf. Section 2.2). We furthermore consider a nominal model with parameter values $\boldsymbol{\theta} = [0 \ 0]^\top$, so that the problem presents a structural mismatch. The modified optimization problem that is solved at each iteration to determine the next RTO move is thus given by:

$$\begin{aligned} \mathbf{d}^{k+1} \in \arg \min_{\mathbf{d}} \quad & \mathcal{A}[y_1 + \mu_{\delta y_1}^k, \sigma_{\delta y_1}^k, \cdot](\mathbf{u}^k + \mathbf{d}) \\ \text{s.t.} \quad & [y_2 + \mu_{\delta y_2}^k](\mathbf{u}^k + \mathbf{d}) \leq 0 \\ & y_1(\mathbf{u}) := u_1^2 + u_2^2 \\ & y_2(\mathbf{u}) := 1 - u_1 + u_2^2 \end{aligned} \tag{13}$$

where the GP modifiers capture the output mismatch, $y_i^p - y_i \sim \mathcal{GP}(\mu_{\delta y_i}, \sigma_{\delta y_i}^2)$, for $i = 1, 2$; and the acquisition function \mathcal{A} may either be LCB or EI (cf. Section 2.2) or the cost predictor itself ($y_1 + \mu_{\delta y_1}^k$) if exploration is not considered.

On the Benefit of Using an Acquisition Function A key feature of Algorithm 1 lies in the use of an acquisition function for promoting exploration within the active trust region, rather than enforcing full linearity of the surrogate models in Problem (9). The behavior of several modifier-adaptation schemes, without and with such an acquisition function, is compared in Figure 2 for multiple realizations of the process noise.

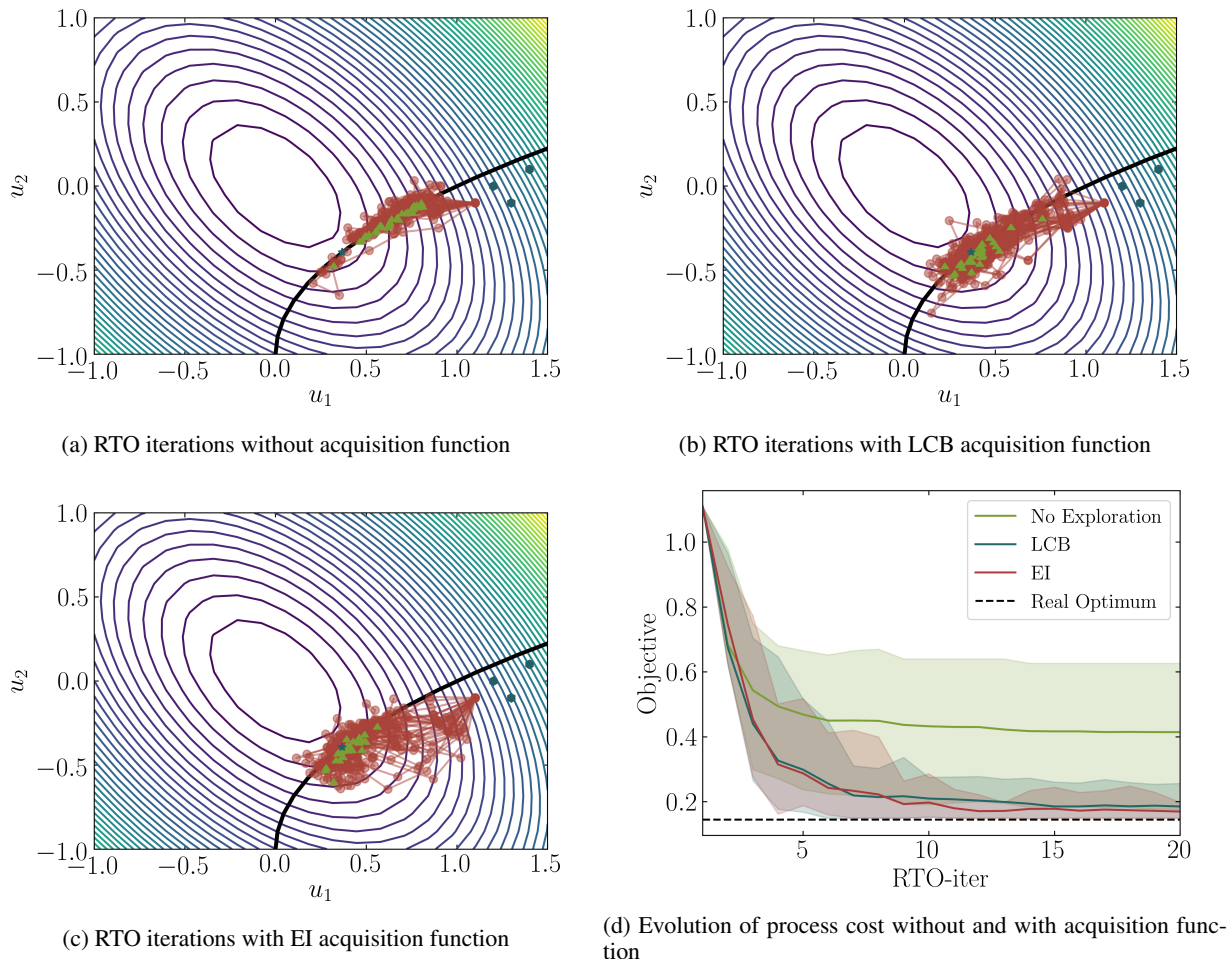


Figure 2: RTO iterations for Problem (12) corresponding to various exploration strategies in Algorithm 1. A prior process model is used and no prior knowledge of the process noise is assumed. **(a), (b), (c)** Clouds of iterates (red connected circles) for 30 process noise realizations, initialized from the same sample points (blue hexagons) and interrupted after 20 RTO iterations (green triangles); the process optimum is depicted with a blue star. **(d)** Evolution of the 95th percentile of process cost values over all the noise realizations with the RTO iterations (showing only the feasible iterates).

The comparison of multiple modifier-adaptation runs on Figure 2a and the corresponding cost envelope on Figure 2d clearly show that, without adding an exploration term in the modified cost of Problem (13), certain RTO runs may get trapped at a suboptimal point. This behavior was not observed under noiseless conditions and is thus attributed to the presence of process noise. A possible cause could be the lack of a model-improvement step and enforcement of full linearity in Algorithm 1 (cf. Appendix A).

By contrast, with the modifier-adaptation schemes that use either the LCB or EI acquisition function (Figures 2b & 2c), the iterates are much more likely to converge to the plant optimum in the presence of noise. This confirms the benefit of adding excitation in the modified cost of the RTO subproblems and that the selected acquisition functions are indeed suitable. Notice that the paths followed by the iterates of both schemes are comparable, although EI seems to drive the iterates more into the interior of the feasible region on this particular example. The comparison between LCB and EI on Figure 2d also suggests that the latter may promote a faster progress and a lower variance around the plant optimum.

On the Benefit of Knowing the Process Noise Not only does GP regression provide a natural approach to describing the plant-model mismatch in a non-parametric way, but it also enables estimating the variance of the observations alongside the other hyperparameters of the GPs in case the noise level is unspecified. In our initial case study shown

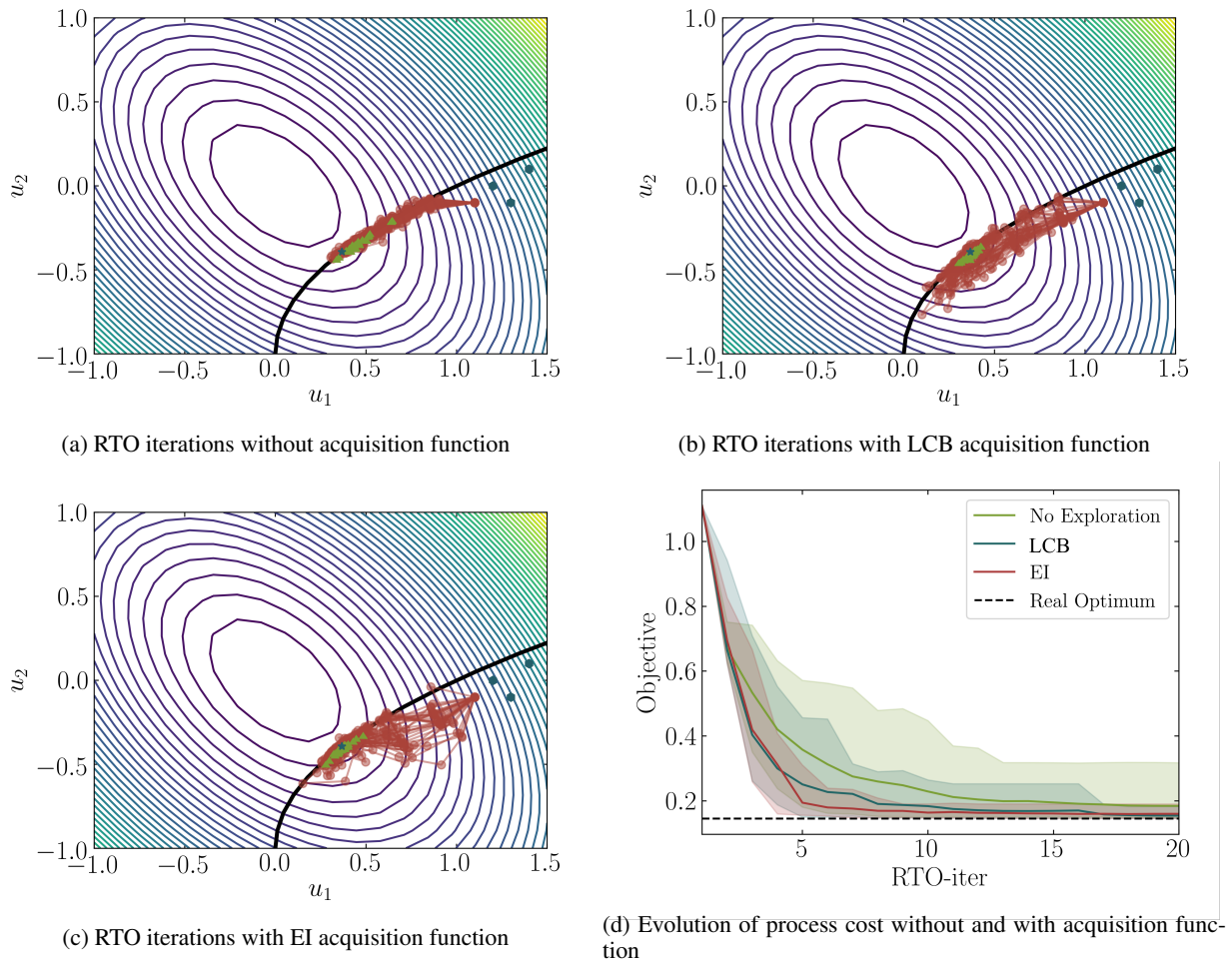


Figure 3: RTO iterations for Problem (12) corresponding to various exploration strategies in Algorithm 1. A prior process model is used and the process noise level is assumed to be given. **(a), (b), (c)** Clouds of iterates (red connected circles) for 30 process noise realizations, initialized from the same sample points (blue hexagons) and interrupted after 20 RTO iterations (green triangles); the process optimum is depicted with a blue star. **(d)** Evolution of the 95th percentile of process cost values over all the noise realizations with the RTO iterations (showing only the feasible iterates).

in Figure 2, we did not assume any prior knowledge of the process noise. By contrast, the results in Figure 3 assume that the (correct) process noise is given.

By and large, the performance of all three modifier-adaptation schemes is clearly enhanced by the specification of the noise level. In the case that no extra excitation is added to the modified cost of the RTO subproblems (Figure 3a), the odds of the iterates getting trapped at a suboptimal point are significantly reduced, albeit still not negligible; while with an acquisition function (Figures 3b & 3c), the variability of the iterates around the plant optimum is much lower. This cursory comparison illustrates well the benefits of characterizing the process noise, e.g. based on historical data.

On the Benefit of Specifying a Nominal Process Model The basic idea behind modifier adaptation entails correcting a model-based optimization problem so that its solution will match the plant optimum upon convergence. By contrast, Bayesian optimization and derivative-free optimization do not rely on a preexisting model, so it seems legitimate to raise the question whether a GP model alone would be suitable to drive such an RTO system. Discarding the process model altogether is akin to model-free RTO, which is easier to design and maintain, but could result in large performance loss or lesser reliability compared to model-based RTO nonetheless. The behavior of a modifier-adaptation scheme without a prior (nominal) model—that is, setting $y_1(\mathbf{u}) = y_2(\mathbf{u}) = 0$ in Problem (13)—is shown in Figure 4.

The cloud of iterates on Figure 4a presents a much larger span than its counterpart on Figure 2c which uses a prior model and the same EI acquisition function. This behavior is also observed on Figure 4b where the envelope of cost values for a range of noise scenarios is two to three times wider after discarding the nominal process model. Many more infeasible iterates are furthermore generated in this latter scenario, which requires backing-off more frequently and thereby slows down the adaptation. The fact that several final iterates are not on the constraint in Figure 4a suggests that, without building on a prior model, the GP surrogates yield an inaccurate prediction of the actual process constraint. The reason for this could be the lack of exploration of the feasible region, since an acquisition function is only used to promote exploration in the objective function of Problem (13). Improved modifier-adaptation schemes that add excitation to both the cost and constraint functions will be investigated in future work.

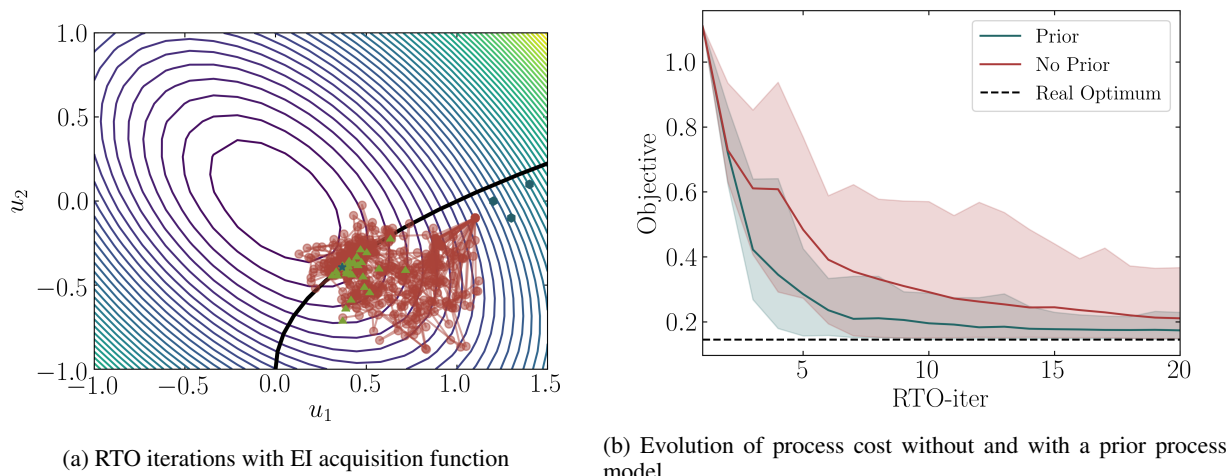


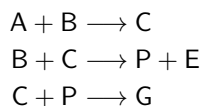
Figure 4: RTO iterations for Problem (12) generated by Algorithm 1 without and with a prior model. The EI acquisition function is used and no prior knowledge of the process noise is assumed. **(a)** Clouds of iterates (red connected circles) for 30 process noise realizations, initialized from the same sample points (blue hexagons) and interrupted after 20 RTO iterations (green triangles); the process optimum is depicted with a blue star. **(b)** 95th percentile of the process cost values over all noise realizations at each RTO iteration (showing only the feasible iterates).

Overall, the comparisons conducted in this section have provided compelling evidence that (i) using an acquisition function, (ii) knowing the process noise level, and (iii) specifying a nominal process model can greatly enhance the reliability of a modifier-adaptation scheme based on GP modifiers. Naturally, the extent to which such design choices will improve an RTO system is largely problem dependent. The following section presents further results for two numerical case studies.

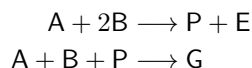
4 Case Studies

4.1 Williams-Otto Benchmark Problem

We first assess the proposed modifier-adaptation algorithm with Gaussian process, trust region and acquisition function (Algorithm 1) on the classical Williams-Otto benchmark problem. A continuous stirred-tank reactor (CSTR) is fed with two streams of pure components A and B, with respective mass flowrates F_A and F_B . The reactor operates at steady state and under the temperature T_r . The chemical reactions between these reagents produce two main products P and E, through a series of chemical reactions that also produce an intermediate C and a byproduct G:



Structural plant-model mismatch is introduced in the problem by assuming that the approximate kinetic model only knows about the following two reactions, which omit the intermediate species C:



The complete set of mass-balance equations and kinetic rate equations for both reaction systems are the same as those reported by Mendoza et al. (2016) and not reproduced here for brevity.

The optimization problem seeks to maximize the economic profit by manipulating the feedrate F_B and the reactor temperature T_r , subject to operating constraints on the residual mass fractions of A and G at the reactor outlet:

$$\begin{aligned} \min_{F_B, T_r} \quad & G_0 := (1043.38X_P + 20.92X_E)(F_A + F_B) - 79.23F_A - 118.34F_B \quad (14) \\ \text{s.t.} \quad & \text{CSTR model (Mendoza et al., 2016)} \\ & G_1 := X_A - 0.12 \leq 0 \\ & G_2 := X_G - 0.08 \leq 0 \\ & F_B \in [4, 7], \quad T_r \in [70, 100] \end{aligned}$$

where X_i denotes the mass fraction of species i . A graphical depiction of the problem (14) is presented in Figure 5, where both the contour levels of the plant cost (thin multicolored lines) and the plant constraint limits (thick black lines) are shown. The case study furthermore assumes that measurements for the cost and constraint functions are available, corrupted by Gaussian distributed noise with zero mean and standard deviation $\sigma_{G_0} = 0.5$, $\sigma_{G_1} = \sigma_{G_2} = 0.0005$. However, no prior knowledge of this noise level is assumed during the construction of the GP surrogates.

The python code used to solve this case study is made available as part of the Supporting Information. The NLP solver IPOPT (Wächter and Biegler, 2006) is used to solve the optimization subproblems in the modifier-adaptation scheme. It is combined with a simple multistart heuristic (20 random starting points) to overcome numerical failures of the NLP solver and reduce the likelihood of converging to a local optimum.

An illustration of the trust-region evolution along a particular RTO run is presented in Figure 5a. During the first few iterations Algorithm 1 follows a straight path and increases the trust-region radius Δ , until the boundary of the feasible domain is reached. After that, the iterates follow the active constraint and the trust-region radius is reduced to prevent constraint violations. Here, both constraints are considered unrelaxable ($\mathcal{UC} = \{1, 2\}$) and Δ is reduced by a factor of 0.8 in Step 4 after back-tracking from any infeasible move. The iterates reach a close neighborhood of the plant optimum where both constraints are active after about 10 iterations.

A comparison between multiple modifier-adaptation runs with either the LCB or EI acquisition function is presented in Figure 5b. The performance is comparable and all the runs reach a neighborhood of the plant optimum within 7–11 iterations, after which they remain in the level of noise. The corresponding clouds of iterates on Figures 5c & 5d confirm this rapid convergence, despite several constraint violations during the search. Some of the final points after 20 iterations (green triangles) appear to be quite distant from the plant optimum, which is caused by the low sensitivity of the cost along one of the active constraints in comparison to the noise level; that is, the iterates do not get stuck at a suboptimal point.

Finally, it is worth pointing out that the performance of Algorithm 1 on this benchmark problem, both in terms of speed and reliability, is comparable that of other modifier-adaptation schemes. this includes the approach by Gao et al. (2016) which combines modifier adaptation with quadratic surrogates and the nested modifier-adaptation approach by Navia et al. (2015).

4.2 Batch-to-Batch Bioreactor Optimization

Our final case study investigates the performance of the proposed methodology in higher-dimensional RTO problems. We consider the batch-to-batch optimization of a photobioreactor for the production of phycocyanin (P) by the blue-green cyanobacterium *Arthrospira platensis* (X) growing on nitrates (N). A dynamic model describing the concentrations C_X [g L^{-1}], C_N [mg L^{-1}] and C_P [mg L^{-1}] in the photobioreactor is given by (Bradford et al., 2020):

$$\dot{C}_X(t) = u_m \frac{I(t)}{I(t) + k_s + I(t)^2/k_i} \frac{C_N(t)}{C_N(t) + K_N} C_X(t) - u_d C_X(t) \quad (15)$$

$$\dot{C}_N(t) = -Y_{N/X} u_m \frac{I(t)}{I(t) + k_s + I(t)^2/k_i} \frac{C_N(t)}{C_N(t) + K_N} C_X(t) + F_N(t) \quad (16)$$

$$\dot{C}_P(t) = k_m \frac{I(t)}{I(t) + k_{sq} + I(t)^2/k_{iq}} C_X(t) - k_d \frac{C_P(t)}{C_N(t) + K_{Np}} \quad (17)$$

where the light intensity $I(t)$ [$\mu\text{E m}^2 \text{s}^{-1}$] and the nitrate inflow rate $F_N(t)$ [$\text{mg L}^{-1} \text{h}^{-1}$] are manipulated inputs; and the values of the model parameters k_d , k_m , k_s , k_i , k_{sq} , k_{iq} , K_N , K_{Np} , u_d , u_m , $Y_{N/X}$ are the same as those reported by Bradford et al. (2020). For simplicity, the mass-balance equations (15)–(17) neglect the change in volume due to the nitrate addition and the kinetic model assumes nutrient-replete growth conditions.

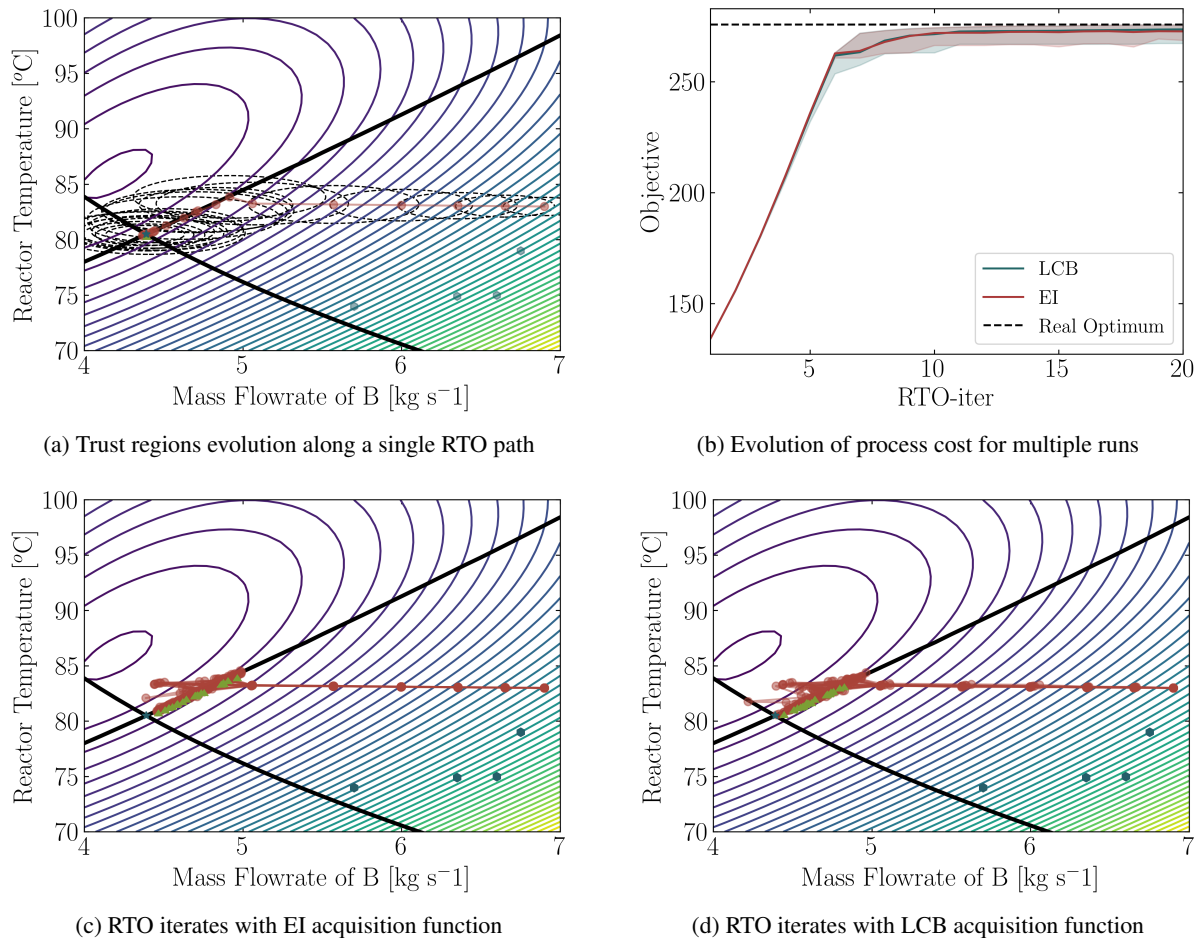


Figure 5: RTO results for the Williams-Otto case study (Problem 14) using Algorithm 1. **(a)** Evolution of the trust-region size (dashed ellipsoids) for a single RTO run with EI acquisition function, interrupted after 20 iterations. **(b)** Evolution of the 95th percentile of process cost values over 30 noise realizations with the RTO iterations (showing only the feasible iterates). **(c)**, **(d)** Clouds of iterates (red connected circles) for 30 process noise realizations, initialized from the same sample points (blue hexagons) and interrupted after 20 RTO iterations (green triangles); the process optimum is depicted with a blue star.

The optimization problem seeks to maximize the end-batch concentration of phycocyanin after 240 hours of operation. Regarding constraints, the phycocyanin-to-cyanobacterial-biomass ratio must be kept under 1.1 wt% at all times; the nitrate concentration must be kept under 800 mg L⁻¹ at all times and below 150 mg L⁻¹ at the end of the batch; and both manipulated inputs are bounded. A mathematical formulation of this (dynamic) optimization problem is as follows:

$$\begin{aligned}
 & \min_{I(t), F_N(t)} C_P(240) & (18) \\
 & \text{s.t. PBR model (15)–(17)} \\
 & C_X(0) = 1, C_N(0) = 150, C_P(0) = 0 \\
 & C_P(t) \leq 0.011C_X(t), \forall t \\
 & C_N(t) \leq 800, \forall t \\
 & C_N(240) \leq 150 \\
 & 120 \leq I(t) \leq 400, \forall t \\
 & 0 \leq F_N(t) \leq 40, \forall t
 \end{aligned}$$

In order to recast it as a finite-dimensional optimization problem, both control trajectories are discretized using a piecewise-constant parameterization over 6 equidistant stages (of 60 hours each). The batch-to-batch optimization

therefore comprises a total of 12 degrees of freedom. The state path constraints are also discretized and enforced at the end of each control stage.

The case study assumes that the concentrations C_X , C_N and C_P can all be measured during or at the end of the batch as necessary. Process noise is simulated in this virtual reality by adding a Gaussian white noise with zero mean and standard deviation $\sigma_{C_X} = 0.02$ [g L⁻¹], $\sigma_{C_N} = 0.316$ [mg L⁻¹], and $\sigma_{C_P} = 0.0001$ [mg L⁻¹]. However, no prior knowledge of this measurement noise is assumed during the construction of the GP surrogates for the cost and constraint defects. We also depart from the previous case studies by using a Matérn kernel (with parameter $\nu = \frac{3}{2}$) instead of the usual squared-exponential kernel (cf. Section 2.2).

Next, Algorithm 1 is applied to solve Problem (18), both without and with the use of a nominal process model. The following dynamic model is used for the latter, which presents a structural mismatch with the plant model (15)–(17) regarding the light inhibition kinetics:

$$\dot{C}_X(t) = u_m \frac{I(t)}{I(t) + k_s} \frac{C_N(t)}{C_N(t) + K_N} C_X(t) - u_d C_X(t) \quad (19)$$

$$\dot{C}_N(t) = -Y_{N/X} u_m \frac{I(t)}{I(t) + k_s} \frac{C_N(t)}{C_N(t) + K_N} C_X(t) + F_N(t) \quad (20)$$

$$\dot{C}_P(t) = k_m \frac{I(t)}{I(t) + k_{sq}} \frac{c_N}{C_N(t) + K_N} C_X(t) - k_d \frac{C_P(t)}{C_N(t) + K_{Np}} \quad (21)$$

For their numerical solutions, the resulting dynamic optimization subproblems are discretized using a 4th-order Runge Kutta scheme over 25 subintervals for each control stage. All of the NLP problems are solved using IPOPT (Wächter and Biegler, 2006) interfaced with CasADi (Andersson et al., 2019) for computing the required derivatives. A simple multistart heuristic (20 random starting points) is applied to overcome the numerical failures of the NLP solver and reduce the likelihood of converging to a local optimum. The python code used to solve this case study is also made available as part of the Supporting Information.

The initial GPs are trained with 13 feasible data points, which were obtained via trial-and-error, and the initial trust region encloses all of these points. All of the constraints are considered unrelaxable in Algorithm 1. But unlike the other case studies, the trust-region radius is not reduced after back-tracking from an infeasible iterate as this was found to significantly hinder the progression of the RTO iterates.

The performance of Algorithm 1 with the nominal model (19)–(21) as prior and with the EI acquisition function is presented in Figure 6a for multiple realizations of the process noise. All of the runs are seen to reach a neighborhood of the plant optimum within 25–40 iterations, which may be considered fast given the large number of manipulated inputs. The optimized input profiles corresponding to $F_N(t)$ and $I(t)$ after 50 iterations are shown in Figures 6c & 6d, respectively, for the same noise realizations. It can be checked that all of these input profiles are indeed in excellent agreement with the plant optimum, the larger variation range for the input $I(t)$ being attributed to its lower sensitivity compared to $F_N(t)$.

For comparison, the performance of the same algorithm without a prior model (model-free RTO) is reported in Figure 6b. Notice that the behavior is now much more inconsistent across the various RTO runs, with certain runs converging to the plant optimum after just 20 iterations, while others failing to reach the plant optimum and remaining vastly suboptimal after 50 iterations. These results confirm that the use of a nominal model in the manner of a prior constitutes an effective derisking strategy in higher-dimensional RTO problems.

5 Conclusions and Future Directions

The main contribution of this paper lies in the development of an improved modifier-adaptation algorithm by integrating ideas from the related fields of Bayesian optimization and derivative-free optimization. On the one hand, trust-region techniques robustify the search by mitigating risk during the exploration and enable building on an established convergence theory, e.g. for unconstrained RTO problems. On the other hand, GPs are ideally suited to capture the plant-model mismatch or process noise in RTO, and a GP's variance estimator can drive the exploration by means of an acquisition function. These benefits have been analyzed and illustrated with numerical case studies, including a challenging batch-to-batch optimization problem with a dozen inputs and a large number of constraints. The paper has also investigated the benefits of embedding a prior (nominal) process model in the RTO scheme, instead of relying entirely on process data as in model-free RTO. The numerical case studies suggest that embedding a prior model can provide an effective derisking strategy against process noise. In practical applications, this added reliability could outweigh the benefits of model-free RTO, for instance in terms of ease of design and maintainability. Future work will be geared towards improving the reliability of modifier-adaptation RTO schemes further, including the consideration

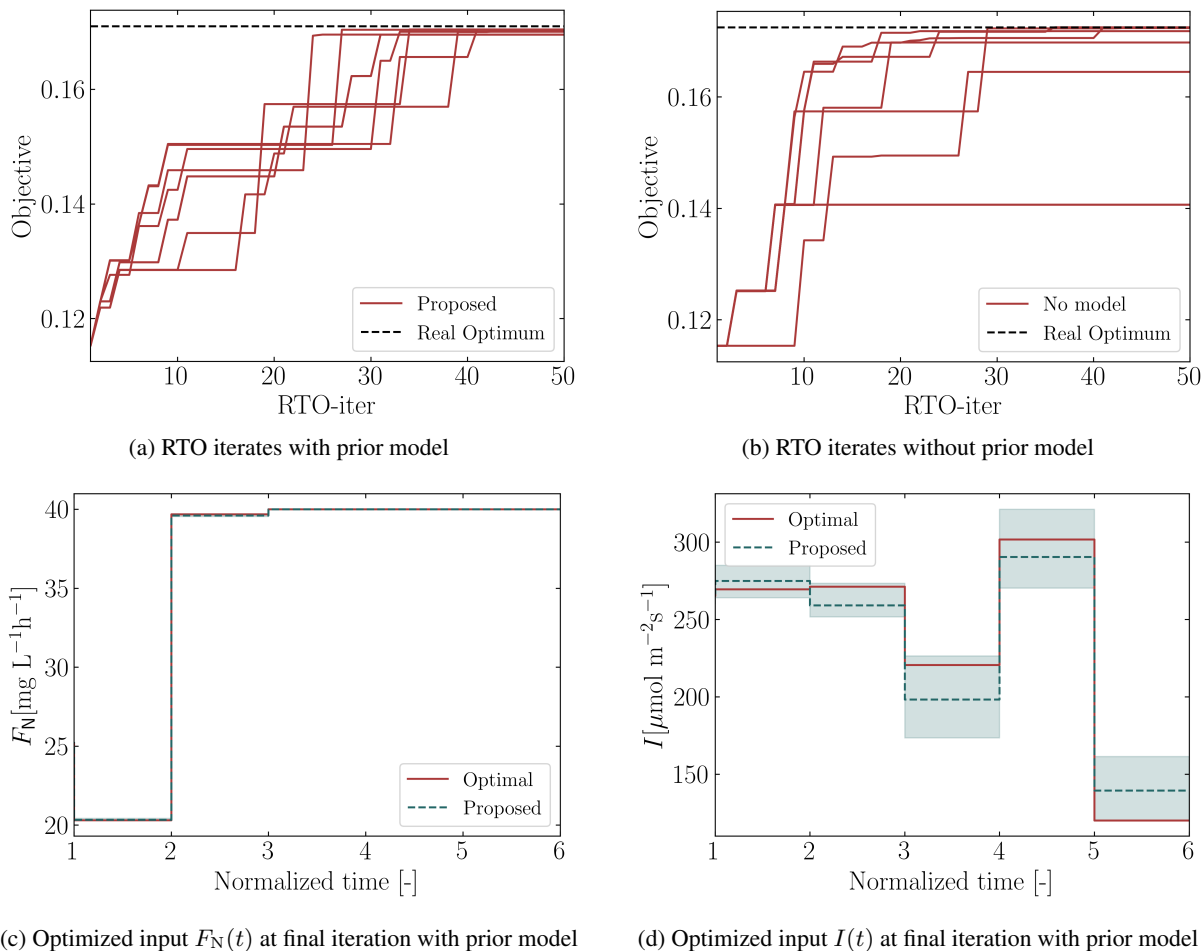


Figure 6: RTO results for the photobioreactor case study (Problem 18) using Algorithm 1. **(a)** Evolution of process cost with the RTO iterations for 8 process noise realizations with the nominal model (19)–(21) used as prior. **(b)** Evolution of process cost with the RTO iterations for 8 process noise realizations without a prior model. Only the feasible iterates are shown. **(c)**, **(d)** Comparison between the optimal inputs $F_N(t)$ and $I(t)$ and the RTO iterates after 50 iterations with the nominal model (19)–(21) used as prior; the envelopes are the same 8 noise realizations as in (a) and the dotted lines show one particular realization.

of acquisition functions for the process constraints in order to promote exploration of the feasible region and accuracy of the GP surrogates. Another promising direction entails incorporating transient information to train the GPs, with a view to enabling dynamic real-time optimization.

Acknowledgements

This paper is based upon work supported by the UK Research and Innovation, and Engineering and Physical Sciences Research Council under grants EP/T000414/1 and EP/P016650/1. Financial support from Shell and FAPESP under grant 2014/50279-4, ANP and CNPq Brasil under grant 200470/2017-5) is gratefully acknowledged. This project has also received funding from the European Union’s Horizon 2020 research and innovation programme under the Marie Skłodowska-Curie grant agreement No 675215.

Supporting Information

The python codes implementing the numerical case studies can be retrieved from the following Git repository: <https://github.com/omega-icl/ma-gp>.

References

- Agrawal, R., 1995. Sample mean based index policies with $O(\log n)$ regret for the multi-armed bandit problem. *Advances in Applied Probability* 27, 1054–1078. doi:10.2307/1427934.
- Andersson, J.A.E., Gillis, J., Horn, G., Rawlings, J.B., Diehl, M., 2019. CasADi – A software framework for nonlinear optimization and optimal control. *Mathematical Programming Computation* 11, 1–36. doi:10.1007/s12532-018-0139-4.
- Audet, C., Conn, A.R., Le Digabel, S., Peyrega, M., 2018. A progressive barrier derivative-free trust-region algorithm for constrained optimization. *Computational Optimization & Applications* 71, 307–329. doi:10.1007/s10589-018-0020-4.
- Audet, C., Dennis, J.E., 2006. Mesh adaptive direct search algorithms for constrained optimization. *SIAM Journal on Optimization* 17, 188–217. doi:10.1137/040603371.
- Augustin, F., Marzouk, Y.M., 2014. NOWPAC: A provably convergent derivative-free nonlinear optimizer with path-augmented constraints. arXiv:1403.1931.
- Bajaj, I., Iyer, S.S., Hasan, M.M.F., 2018. A trust region-based two phase algorithm for constrained black-box and grey-box optimization with infeasible initial point. *Computers & Chemical Engineering* 116, 306–321. doi:10.1016/j.compchemeng.2017.12.011.
- Biegler, L.T., Lang, Y.d., Lin, W., 2014. Multi-scale optimization for process systems engineering. *Computers & Chemical Engineering* 60, 17–30. doi:10.1016/j.compchemeng.2013.07.009.
- Boukouvala, F., Floudas, C.A., 2017. ARGONAUT: AlgoRithms for Global Optimization of coNstrAined grey-box compUTational problems. *Optimization Letters* 11, 895–913. doi:10.1007/s11590-016-1028-2.
- Bradford, E., Imsland, L., del Rio-Chanona, E.A., 2019. Nonlinear model predictive control with explicit back-offs for Gaussian process state space models, in: *Proceedings of 58th Conference on Decision and Control*, pp. 4747–4754. doi:10.1109/CDC40024.2019.9029443.
- Bradford, E., Imsland, L., Zhang, D., del Rio-Chanona, E.A., 2020. Stochastic data-driven model predictive control using Gaussian processes. *Computers & Chemical Engineering* 139, 106844. doi:10.1016/j.compchemeng.2020.106844.
- Bunin, G.A., 2014. On the equivalence between the modifier-adaptation and trust-region frameworks. *Computers & Chemical Engineering* 71, 154–157. doi:10.1016/j.compchemeng.2014.07.028.
- Bunin, G.A., François, G., Bonvin, D., 2013. From discrete measurements to bounded gradient estimates: A look at some regularizing structures. *Industrial & Engineering Chemistry Research* 52, 12500–12513. doi:10.1021/ie303309a.
- Caballero, J.A., Grossmann, I.E., 2008. An algorithm for the use of surrogate models in modular flowsheet optimization. *AIChE Journal* 54, 2633–2650. doi:10.1002/aic.11579.
- Câmara, M.M., Quelhas, A.D., Pinto, J.C., 2016. Performance evaluation of real industrial RTO systems. *Processes* 4, 1–20. doi:10.3390/pr4040044.
- Cartis, C., Fiala, J., Marteau, B., Roberts, L., 2019. Improving the flexibility and robustness of model-based derivative-free optimization solvers. *ACM Transactions on Mathematical Software* 45, 32. doi:10.1145/3338517.
- Cartis, C., Roberts, L., Sheridan-Methven, O., 2018. Escaping local minima with derivative-free methods: a numerical investigation. arXiv:1812.11343.
- Chachuat, B., Srinivasan, B., Bonvin, D., 2009. Adaptation strategies for real-time optimization. *Computers & Chemical Engineering* 33, 1557–1567. doi:10.1016/j.compchemeng.2009.04.014.
- Conn, A.R., Gould, N.I.M., Toint, P.L., 2000. *Trust-Region Methods*. MPS-SIAM Series on Optimization.
- Conn, A.R., Scheinberg, K., Vicente, L.N., 2009a. Global convergence of general derivative-free trust-region algorithms to first-and second-order critical points. *SIAM Journal on Optimization* 20, 387–415. doi:10.1137/060673424.
- Conn, A.R., Scheinberg, K., Vicente, L.N., 2009b. *Introduction to Derivative-Free Optimization*. MOS-SIAM Series on Optimization. doi:10.1137/1.9780898718768.
- Costa, A., Nannicini, G., 2018. RBFOpt: an open-source library for black-box optimization with costly function evaluations. *Mathematical Programming Computation* 10, 597–629. doi:10.1007/s12532-018-0144-7.
- Costello, S., Franois, G., Bonvin, D., 2016. A directional modifier-adaptation algorithm for real-time optimization. *Journal of Process Control* 39, 64–76. doi:10.1016/j.jprocont.2015.11.008.

- Darby, M.L., Nikolaou, M., Jones, J., Nicholson, D., 2011. RTO: An overview and assessment of current practice. *Journal of Process Control* 21, 874–884. doi:10.1016/j.jprocont.2011.03.009.
- Eason, J.P., Biegler, L.T., 2016. A trust region filter method for glass box/black box optimization. *AIChE Journal* 62, 3124–3136. doi:10.1002/aic.15325.
- Eason, J.P., Biegler, L.T., 2018. Advanced trust region optimization strategies for glass box/black box models. *AIChE Journal* 64, 3934–3943. doi:10.1002/aic.16364.
- Echebest, N., Schuverdt, M.L., Vignau, R.P., 2017. An inexact restoration derivative-free filter method for nonlinear programming. *Computational & Applied Mathematics* 36, 693–718. doi:10.1007/s40314-015-0253-0.
- Engell, S., 2007. Feedback control for optimal process operation. *Journal of Process Control* 17, 203–219. doi:10.1016/j.jprocont.2006.10.011.
- Feng, X., Houska, B., 2018. Real-time algorithm for self-reflective model predictive control. *Journal of Process Control* 65, 68–77. doi:10.1016/j.jprocont.2017.10.003.
- Ferreira, T.d.A., Shukla, H.A., Faulwasser, T., Jones, C.N., Bonvin, D., 2018. Real-time optimization of uncertain process systems via modifier adaptation and Gaussian processes, in: *Proceedings of European Control Conference*, pp. 465–470. doi:10.23919/ECC.2018.855039.
- Forbes, J.F., Marlin, T.E., MacGregor, J.F., 1994. Model adequacy requirements for optimizing plant operations. *Computers & Chemical Engineering* 18, 497–510. doi:10.1016/0098-1354(93)E0005-T.
- François, G., Bonvin, D., 2014. Use of transient measurements for the optimization of steady-state performance via modifier adaptation. *Industrial & Engineering Chemistry Research* 53, 5148–5159. doi:10.1021/ie401392s.
- Frazier, P., Powell, W., Dayanik, S., 2009. The knowledge-gradient policy for correlated normal beliefs. *INFORMS Journal on Computing* 21, 599–613. doi:10.1287/ijoc.1080.0314.
- Gao, W., Engell, S., 2005. Iterative set-point optimization of batch chromatography. *Computers & Chemical Engineering* 29, 1401–1409. doi:10.1016/j.compchemeng.2005.02.035.
- Gao, W., Wenzel, S., Engell, S., 2016. A reliable modifier-adaptation strategy for real-time optimization. *Computers & Chemical Engineering* 91, 318–328. doi:10.1016/j.compchemeng.2016.03.019.
- Gutmann, H.M., 2001. A radial basis function method for global optimization. *Journal of Global Optimization* 19, 201–227. URL: <https://doi.org/10.1007/s12532-018-0144-7>, doi:10.1023/A:1011255519438.
- Heirung, T.A.N., Foss, B., Ydstie, B.E., 2015. MPC-based dual control with online experiment design. *Journal of Process Control* 32, 64–76. doi:10.1016/j.jprocont.2015.04.012.
- Heno, C.A., Maravelias, C.T., 2011. Surrogate-based superstructure optimization framework. *AIChE Journal* 57, 1216–1232. doi:10.1002/aic.12341.
- Hennig, P., Schuler, C.J., 2012. Entropy search for information-efficient global optimization. *Journal of Machine Learning Research* 13, 1809–1837. doi:10.5555/2188385.2343701.
- Hewing, L., Wabersich, K.P., Menner, M., Zeilinger, M.N., 2020. Learning-based model predictive control: Toward safe learning in control. *Annual Review of Control, Robotics, and Autonomous Systems* 3, 269–296. doi:10.1146/annurev-control-090419-075625.
- Huang, D., Allen, T.T., Notz, W.I., Miller, R.A., 2006. Sequential kriging optimization using multiple-fidelity evaluations. *Structural and Multidisciplinary Optimization* 32, 369–382. doi:10.1007/s00158-005-0587-0.
- Jeong, D.H., Lee, C.J., Lee, J.M., 2018. Experimental gradient estimation of multivariable systems with correlation by various regression methods and its application to modifier adaptation. *Journal of Process Control* 70, 65–79. doi:10.1016/j.jprocont.2018.08.008.
- Jones, D.R., Schonlau, M., Welch, W.J., 1998. Efficient global optimization of expensive black-box functions. *Journal of Global optimization* 13, 455–492. doi:10.1023/A:1008306431147.
- Keßler, T., Kunde, C., McBride, K., Mertens, N., Michaels, D., Sundmacher, K., Kienle, A., 2019. Global optimization of distillation columns using explicit and implicit surrogate models. *Chemical Engineering Science* 197, 235–245. doi:10.1016/j.ces.2018.12.002.
- Kim, J.W., Park, B.J., Yoo, H., Oh, T.H., Lee, J.H., Lee, J.M., 2020. A model-based deep reinforcement learning method applied to finite-horizon optimal control of nonlinear control-affine system. *Journal of Process Control* 87, 166–178. doi:10.1016/j.jprocont.2020.02.003.
- Klimasauskas, C.C., 1998. Hybrid modeling for robust nonlinear multivariable control. *ISA Transactions* 37, 291–297. doi:10.1016/S0019-0578(98)00030-5.

- Kocijan, J., Murray-Smith, R., Rasmussen, C.E., Girard, A., 2004. Gaussian process model based predictive control, in: *Proceeding of American Control Conference*, pp. 2214–2219.
- Krige, D.G., 1951. A statistical approach to some mine valuations and allied problems at the Witwatersrand. Ph.D. thesis. University of Witwatersrand.
- Krishnamoorthy, D., Foss, B., Skogestad, S., 2018. Steady-state real-time optimization using transient measurements. *Computers & Chemical Engineering* 115, 34–45. doi:10.1016/j.compchemeng.2018.03.021.
- Kushner, H.J., 1964. A new method of locating the maximum point of an arbitrary multipeak curve in the presence of noise. *Journal of Basic Engineering* 86, 97–106. doi:10.1115/1.3653121.
- Lai, T.L., Robbins, H., 1985. Asymptotically efficient adaptive allocation rules. *Advances in Applied Mathematics* 6, 4–22. doi:10.1016/0196-8858(85)90002-8.
- Larson, J., Menickelly, M., Wild, S.M., 2019. Derivative-free optimization methods. *Acta Numerica* 28, 287–404. doi:10.1017/S0962492919000060.
- Larsson, C.A., Annergren, M., Hjalmarsson, H., Rojas, C.R., Bombois, X., Mesbah, A., Modén, P.E., 2013. Model predictive control with integrated experiment design for output error systems, in: *Proceedings of European Control Conference*, pp. 3790–3795. doi:10.23919/ECC.2013.6669533.
- Maiworm, M., Limon, D., Manzano, J.M., Findeisen, R., 2018. Stability of Gaussian process learning based output feedback model predictive control. *IFAC-PapersOnLine* 51, 455–461. doi:10.1016/j.ifacol.2018.11.047.
- Marafioti, G., Bitmead, R.R., Hovd, M., 2014. Persistently exciting model predictive control. *International Journal of Adaptive Control & Signal Processing* 28, 536–552. doi:10.1002/acs.2414.
- March, A., Willcox, K., 2012a. Constrained multifidelity optimization using model calibration. *Structural & Multidisciplinary Optimization* 46, 93–109. doi:10.1007/s00158-011-0749-1.
- March, A., Willcox, K., 2012b. Provably convergent multifidelity optimization algorithm not requiring high-fidelity derivatives. *AIAA Journal* 50, 1079–1089. doi:10.2514/1.J051125.
- Marchetti, A., Chachuat, B., Bonvin, D., 2009. Modifier-adaptation methodology for real-time optimization. *Industrial & Engineering Chemistry Research* 48, 6022–6033. doi:10.1021/ie801352x.
- Marchetti, A., Chachuat, B., Bonvin, D., 2010. A dual modifier-adaptation approach for real-time optimization. *Journal of Process Control* 20, 1027–1037. doi:10.1016/j.jprocont.2010.06.006.
- Marchetti, A., François, G., Faulwasser, T., Bonvin, D., 2016. Modifier adaptation for real-time optimization – Methods and applications. *Processes* 4, 55.
- Marlin, T.E., Hrymak, A.N., 1997. Real-time operations optimization of continuous processes, in: *AIChE Symposium Series - CPC-V*, pp. 156–164.
- Mendoza, D.F., Graciano, J.E.A., Liporace, F.S., Le Roux, G.A.C., 2016. Assessing the reliability of different real-time optimization methodologies. *The Canadian Journal of Chemical Engineering* 94, 485–497.
- Močkus, J., 1975. On Bayesian methods for seeking the extremum, in: Marchuk, G.I. (Ed.), *Optimization Techniques IFIP Technical Conference Novosibirsk, July 1–7, 1974*, Springer, Berlin. pp. 400–404. doi:10.1007/3-540-07165-2_55.
- Navia, D., Briceño, L., Gutiérrez, G., de Prada, C., 2015. Modifier-adaptation methodology for real-time optimization reformulated as a nested optimization problem. *Industrial & Engineering Chemistry Research* 54, 12054–12071. doi:10.1021/acs.iecr.5b01946.
- Petsagkourakis, P., Sandoval, I.O., Bradford, E., Galvanin, F., Zhang, D., del Rio-Chanona, E.A., 2020a. Chance constrained policy optimization for process control and optimization. *arXiv:2008.00030*.
- Petsagkourakis, P., Sandoval, I.O., Bradford, E., Zhang, D., del Rio-Chanona, E.A., 2020b. Reinforcement learning for batch bioprocess optimization. *Computers & Chemical Engineering* 133, 106649. doi:10.1016/j.compchemeng.2019.106649.
- Petsagkourakis, P., Sandoval, I.O., Bradford, E., Zhang, D., del Rio Chanona, E.A., 2020c. Constrained reinforcement learning for dynamic optimization under uncertainty. *arXiv:2006.02750*.
- Piche, S., Sayyar-Rodsari, B., Johnson, D., Gerules, M., 2000. Nonlinear model predictive control using neural networks. *IEEE Control Systems Magazine* 20, 53–62. doi:10.1109/37.845038.
- Picheny, V., Gramacy, R.B., Wild, S., Le Digabel, S., 2016. Bayesian optimization under mixed constraints with a slack-variable augmented Lagrangian, in: Lee, D.D., Sugiyama, M., Luxburg, U.V., Guyon, I., Garnett, R. (Eds.), *Advances in Neural Information Processing Systems 29: Annual Conference on Neural Information Processing Systems 2016, December 5–10, 2016, Barcelona, Spain*, pp. 1435–1443.

- Powell, B.K.M., Machalek, D., Quah, T., 2020. Real-time optimization using reinforcement learning. *Computers & Chemical Engineering* 143, 107077. doi:10.1016/j.compchemeng.2020.107077.
- Quirante, N., Javaloyes, J., Caballero, J., 2015. Rigorous design of distillation columns using surrogate models based on kriging interpolation. *AIChE Journal* 61, 2169–2187. doi:10.1002/aic.14798.
- Rasmussen, C.E., Williams, C.K.I., 2016. *Gaussian Processes for Machine Learning*. MIT Press.
- Rawlings, J.B., Mayne, D.Q., Diehl, M.M., 2017. *Model Predictive Control: Theory, Computation, and Design*. 2nd ed., Nob Hill Publishing.
- del Rio-Chanona, E.A., Alves Graciano, J.E., Bradford, E., Chachuat, B., 2019. Modifier-adaptation schemes employing gaussian processes and trust regions for real-time optimization. *IFAC-PapersOnLine* 52, 52–57. doi:10.1016/j.ifacol.2019.06.036.
- Rodger, E.A., Chachuat, B., 2011. Design methodology of modifier adaptation for on-line optimization of uncertain processes. *IFAC Proceedings Volumes* 44, 4113–4118. doi:10.3182/20110828-6-IT-1002.01055.
- Schweidtmann, A.M., Bongartz, D., Grothe, D., Kerkenhoff, T., Lin, X., Najman, J., Mitsos, A., 2020. Global optimization of Gaussian processes. *arXiv:2005.10902*.
- Shahriari, B., Swersky, K., Wang, Z., Adams, R.P., de Freitas, N., 2016. Taking the human out of the loop: A review of Bayesian optimization. *Proceedings of the IEEE* 104, 148–175. doi:10.1109/JPROC.2015.2494218.
- Singhal, M., Marchetti, A.G., Faulwasser, T., Bonvin, D., 2016. Real-time optimization based on adaptation of surrogate models. *IFAC-PapersOnLine* 49, 412–417. doi:10.1016/j.ifacol.2016.07.377.
- Snoek, J., Larochelle, H., Adams, R.P., 2012. Practical Bayesian optimization of machine learning algorithms, in: *Proceedings of 25th International Conference on Neural Information Processing Systems*, Curran Associates Inc., Red Hook (NY). pp. 2951–2959.
- Speakman, J., François, G., 2020. Real-time optimization via modifier adaptation of closed-loop processes using transient measurements. *Computers & Chemical Engineering* 140, 106969. doi:10.1016/j.compchemeng.2020.106969.
- Spielberg, S., Tulsyan, A., Lawrence, N.P., Loewen, P.D., Gopaluni, B.R., 2019. Toward self-driving processes: A deep reinforcement learning approach to control. *AIChE Journal* 65, e16689. doi:10.1002/aic.16689.
- Srinivas, N., Krause, A., Kakade, S., Seeger, M., 2010. Gaussian process optimization in the bandit setting: No regret and experimental design, in: *Proceedings of 27th International Conference on International Conference on Machine Learning*, Omnipress, Madison (WI). pp. 1015–1022. doi:10.5555/3104322.3104451.
- von Stosch, M., Oliveira, R., Peres, J., Feyo de Azevedo, S.a., 2014. Hybrid semi-parametric modeling in process systems engineering: Past, present and future. *Computers & Chemical Engineering* 60, 86–101. doi:10.1016/j.compchemeng.2013.08.008.
- Tatjewski, P., 2002. Iterative optimizing set-point control – The basic principle redesigned. *IFAC Proceedings Volumes* 35, 49–54. doi:10.3182/20020721-6-ES-1901.00994.
- Tejeda-Iglesias, M., Lappas, N.H., Gounaris, C.E., Ricardez-Sandoval, L., 2019. Explicit model predictive controller under uncertainty: An adjustable robust optimization approach. *Journal of Process Control* 84, 115–132. doi:10.1016/j.jprocont.2019.09.002.
- Thompson, M.L., Kramer, M.A., 1994. Modeling chemical processes using prior knowledge and neural networks. *AIChE Journal* 40, 1328–1340. doi:10.1002/aic.690400806.
- Törn, A., Žilinskas, A., 1989. *Global Optimization*. volume 350 of *Lecture Notes in Computer Science*. Springer-Verlag, Berlin, Germany. doi:10.1007/3-540-50871-6.
- Wächter, A., Biegler, L.T., 2006. On the implementation of an interior-point filter line-search algorithm for large-scale nonlinear programming. *Mathematical Programming* 106, 25–57. doi:10.1007/s10107-004-0559-y.
- Wild, S.M., Regis, R.G., Shoemaker, C.A., 2008. ORBIT: Optimization by radial basis function interpolation in trust-regions. *SIAM Journal on Scientific Computing* 30, 3197–3219. doi:10.1137/070691814.
- Wilson, Z.T., Sahinidis, N.V., 2017. The ALAMO approach to machine learning. *Computers & Chemical Engineering* 106, 785–795. doi:10.1016/j.compchemeng.2017.02.010.
- Wittenmark, B., 1995. Adaptive dual control methods: An overview. *IFAC Proceedings Volumes* 28, 67–72. doi:10.1016/B978-0-08-042375-3.50010-X.
- Wu, Z., Tran, A., Rincon, D., Christofides, P.D., 2019. Machine learning-based predictive control of nonlinear processes. Part I: Theory. *AIChE Journal* 65, e16729. doi:10.1002/aic.16729.

Zhang, Z., Wu, Z., Rincon, D., Christofides, P.D., 2019. Real-time optimization and control of nonlinear processes using machine learning. *Mathematics* 7, 890. doi:10.3390/math7100890.

Appendix A. Global Convergence in Unconstrained RTO Problems

This appendix formalizes the global convergence properties of Algorithm 1 to a first-order critical point in unconstrained RTO problems. In this setup, the reduced gradient (Step 1) corresponds to the modified cost gradient $\nabla[G_0 + \mu_{\delta G_0}^k]$; the acquisition function of the optimization subproblems (Step 2) is simply the modified cost $[G_0 + \mu_{\delta G_0}^k]$; the process measurements (Step 3) are noiseless; and $n_g = 0$ so the feasibility test (Step 4) is not needed. Building on established convergence theory from the field of derivative-free optimization (Conn et al., 2009b, Chapter 10), a set of sufficient conditions relies on the following assumptions:

Assumption A.1. *The process cost G_0^p is continuously differentiable with Lipschitz continuous gradient and bounded from below on the neighborhood $\bigcup_{\mathbf{u} \in \mathcal{U}} \mathcal{B}(\mathbf{u}; \Delta_{\max})$ of the input domain \mathcal{U} for some radius $\Delta_{\max} > 0$.*

Assumption A.2. *The modified cost $[G_0 + \mu_{\delta G_0}^k]$ is fully linear on $\mathcal{B}(\mathbf{u}^k; \Delta^k)$ at every iteration $k = 0, 1, \dots$ of Algorithm 1; that is, $[G_0 + \mu_{\delta G_0}^k]$ is continuously differentiable with Lipschitz continuous gradient, and there exist global constants $\kappa_{\text{ef}}, \kappa_{\text{eg}} < \infty$ (independent of k) such that:*

$$\begin{aligned} \|\nabla G_0^p(\mathbf{u}^k + \mathbf{d}) - \nabla[G_0 + \mu_{\delta G_0}^k](\mathbf{u}^k + \mathbf{d})\| &\leq \kappa_{\text{eg}} \Delta^k \\ |G_0^p(\mathbf{u}^k + \mathbf{d}) - [G_0 + \mu_{\delta G_0}^k](\mathbf{u}^k + \mathbf{d})| &\leq \kappa_{\text{ef}} (\Delta^k)^2 \end{aligned}$$

for all $\mathbf{d} \in \mathcal{B}(\mathbf{u}^k; \Delta^k)$ and all iterations k .

Theorem A.1. *Under Assumptions A.1 and A.2, the iterates produced by Algorithm 1 for an unconstrained RTO problem with noiseless measurements are globally convergent to a first-order critical point.*

Proof. See Conn et al. (2009b, Theorem 10.13). □

Besides standard smoothness and boundedness assumptions on the process and model cost functions, the key assumption in Theorem A.1 is the need for a fully linear model on every iteration (Assumption A.2). This ensures that the model of the objective function has uniformly good local accuracy, similar in essence to the local behavior of first-order Taylor model. In their multifidelity optimization algorithm, March and Willcox (2012b) also enforced full linearity of the surrogate models on every iteration using a sampling policy developed by Wild et al. (2008). Likewise, the constrained flowsheet optimization algorithm by Eason and Biegler (2016, 2018) posits full linearity of the surrogate models on every iteration.

Unfortunately, enforcing full linearity at every step of an RTO system would involve taking extra samples by perturbing the process in all directions around the current iterate, which is undesirable or even impractical. Though it should be noted that the global convergence property of derivative-free trust-region algorithms may still hold if the models are not fully linear on every iteration, provided that the iterates yield a sufficient decrease in the objective function (Conn et al., 2009a,b). Instead, the main idea in Algorithm 1 is to consider acquisition functions from the field of Bayesian optimization to promote exploration within the trust region (cf. Problem 9). This approach does not come with a formal convergence proof, but its efficiency and reliability can be established with numerical case studies.